JNeurosci
THE JOURNAL OF NEUROSCIENCE

Research Articles | Behavioral/Cognitive

Self-awareness from whole-body movements

https://doi.org/10.1523/JNEUROSCI.0478-24.2024

Received: 19 March 2024
Revised: 14 September 2024
Accepted: 19 October 2024

Self-awareness from whole-body movements

Authors: Akila Kadambi[1]*, Gennady Erlikhman[1], Micah Johnson[1], Martin M. Monti[1,2,3], Marco Iacoboni[2], Hongjing Lu[1,4]

Affiliations:

1. Department of Psychology, University of California Los Angeles, Los Angeles, CA, USA
2. Department of Psychiatry and Biobehavioral Sciences, David Geffen School of Medicine, University of California Los Angeles, Los Angeles, CA, USA
3. Department of Neurosurgery, Brain Research Center, David Geffen School of Medicine, University of California Los Angeles, Los Angeles, CA, USA
4. Department of Statistics, University of California Los Angeles, Los Angeles, CA, USA

***** *Corresponding author:* akadambi@ucla.edu

Abstract
(150 words)

Humans can recognize their whole-body movements even when displayed as dynamic dot patterns. The sparse depiction of whole-body movements, coupled with a lack of visual experience watching ourselves in the world, has long implicated non-visual mechanisms to self-action recognition. We aimed to identify the neural systems for this ability. Using general linear modeling and multivariate analyses on human brain imaging data from male and female participants, we first found that cortical areas linked to motor processes, including frontoparietal and primary somatomotor cortices, exhibit greater engagement and functional connectivity when recognizing self-generated versus other-generated actions. Next, we show that these regions encode self-identity based on motor familiarity, even after regressing out idiosyncratic visual cues using multiple regression representational similarity analysis. Last, we found the reverse pattern for unfamiliar individuals: encoding localized to occipito-temporal visual regions. These findings suggest that self-awareness from actions emerges from the interplay of motor and visual processes.

Significance Statement: We report for the first time that self-recognition from visual observation of our whole-body actions implicates brain regions associated with motor processes. On functional neuroimaging data, we found greater activity and unique representational patterns in brain areas and networks linked to motor processes when viewing our own actions relative to viewing the actions of others. These findings introduce an important role of motor mechanisms in distinguishing the self from others.

Introduction

Self-recognition is possible even from visually minimalistic dot-displays (Johansson, 1973; Cutting & Kozlowski, 1977; Loula et al., 2005). These displays, called point-light displays (PLDs), depict whole-body actions with around a dozen moving dots (Johansson, 1973; Cutting & Kozlowski, 1977; Loula et al., 2005). While glimpses of our whole-bodies may be captured in videos or glass mirrors, they are far less observable than the rich visual experiences we have seeing movements of close friends or family members. Yet, humans recognize their own movements better than familiar others' in PLDs (Loula et al., 2005; Beardsworth & Buckner, 1981). This self-recognition advantage persists across viewpoints (Jokisch et al., 2006; Prasad & Shiffrar, 2009), task judgments (Knoblich & Flach, 2001; Bischoff et al., 2012), body parts (Frassinetti et al., 2009; Daprati & Sirigu, 2002), and action types (Burling et al., 2019; Kadambi et al., 2024), suggesting that self-action recognition relies on modalities more than vision alone. Despite consistent behavioral evidence, the neural mechanisms remain untested, representing a crucial gap in understanding human self-awareness.

Neuroimaging studies in visual neuroscience often omit the self and focus on the neural mechanisms coding other people's actions. These studies show that action recognition engages a distributed network of cortical areas, termed action observation network (AON). This network consists of occipito-temporal (OT) (posterior superior temporal sulcus (pSTS), extrastriate body area, fusiform gyri) and frontoparietal circuits engaged during action production, including inferior parietal lobe (IPL), premotor cortex (PM), inferior frontal cortex (IFC), and supplementary motor area (SMA). The crucial connection between OT and frontoparietal regions is via pSTS-IPL direct connections, bridging action recognition via visual processing with cognitive theories of action simulation (Ürgen et al., 2019; Grèzes et al., 2003).

While OT regions encode actions irrespective of identity, frontoparietal and somatomotor regions may be critical for self-recognition. These regions are attributed action simulation, or mirroring, functions– mapping observed actions onto one's own motor system. For instance, spiking activity from single and multi-units recorded first in frontoparietal regions in macaques (Di Pellegrino et al., 1992; Fogassi et al, 2005) and later in medial frontal cortex (likely pre-SMA) in humans (Mukamel et al., 2010) during action observation show similar activity during action production. This correspondence in spiking activity is further seen with systems-level activity in these regions during brain imaging and is modulated by the observer's motor familiarity with the action (Rizzolatti & Craighero, 2004; Iacoboni, 2009; Calvo-Marino et al., 2006). Since self-generated actions are most motorically familiar, this could be one mechanism to help differentiate self and other actions.

To date, few neuroimaging studies have investigated self-action recognition from PLDs. These studies support frontoparietal involvement, but used isolated body parts (Bischoff et al., 2012; Macuga and Frey, 2011) or actions that were not self-generated, but associated with self-identity (Woźniak et al., 2022). Hence, the neural mechanisms supporting self-recognition of whole-body actions remain untested. Moreover, beyond regional univariate activity, representational markers are needed to elucidate the featural space supporting self-recognition. Using representational similarity analysis (RSA; Kriegeskorte et al., 2008) can be a viable tool to localize and infer the type of information encoded in neural activity patterns.

In the present study, we asked the following: which neural systems underlie self-recognition from whole-body actions? Does self-action recognition rely more on motor mechanisms, even after accounting for distinctive visual features of the actions, as compared to other identities? To address these questions, we conducted a multimodal imaging study across two sessions. In Session 1, we motion-captured a range of actions of participants and their close friend of the same sex. These actions were performed using both visual instruction (imitation) and verbal instruction (freely performed). After a delay period, participants returned in Session 2 for fMRI where they underwent an identity-recognition task on PLDs of themselves, friends, and strangers.

We hypothesized that AON would be involved during action observation for all identities (self, friends, strangers), encoded in occipito-temporal regions. However, we expected that frontoparietal regions associated with motor processes would greater engage for the self, controlling for visual familiarity (friend) and person identity (stranger). Moreover, if these regions encode motor information to achieve self-recognition, then we expected that activity patterns in frontoparietal and motor regions would relate to motor familiarity with actions, captured over and above visual feature contributions.

Materials and Methods

Participants

Twenty right-handed undergraduate participants (M_{age} = 20.55, SD_{age} = 1.73, females = 12, males = 8) were recruited from around the University of California, Los Angeles area using convenience sampling. All participants were provided payment for their participation. Sample size was based on prior fMRI studies most similar to ours using biological motion (e.g., Saygin et al., 2004; Chang et al., 2021; Engelen et al., 2015) and self-generated point-light displays (Bischoff et al., 2012). The study was approved by the UCLA Institutional Review Board. All participants were naïve to the purpose of the study. Participants had normal or corrected-to-normal vision and no physical disabilities.

Apparatus

The Microsoft Kinect V2.0 and Kinect SDK were used for motion-capture of actions, as in previous studies on self-action recognition (Kadambi et al., 2024; Burling et al., 2019). Customized software developed in our lab was used to enhance movement signals, and to carry out additional processing and trimming for actions presented later in the testing phase (Van Boxtel & Lu, 2013). Three-dimensional (X-Y-Z) coordinates of the key joints were extracted at a rate of approximately 33 frames per second. Each action was trimmed to the start and stop of a T-position signaled by the participant and normalized to scale for use in the experimental task. Note that while motion capture accuracy was high, the Kinect occasionally produced noise jittering in the stimuli, where frame-to-frame joints positions occasionally showed sudden jumps in position. Hence, to remove noisy frame-to-frame jitter, we impinged a manual correction for certain frames (i.e., replacing with the closest previous frame where the jitter was not present).

Stimuli

Twelve actions were selected from our previous work on self-action recognition (Burling et al., 2019; Kadambi and Lu, 2019; Kadambi et al., 2024). These actions conveyed a range of variability in terms of action planning. Six of the actions (i.e. *argue, wash windows, get attention, hurry up, stretch, and play guitar)* were categorized as "verbally instructed actions", delineated by a high degree of motor goal complexity as defined in our previous work (Burling et al., 2019; Kadambi et al., 2024). These actions were verbally instructed to the participant (e.g., please perform the action: "to argue"). The remaining six actions were visually instructed (imitation) actions, depicting a range of simple and complex goals (i.e., *jumping jacks, basketball, digging, chopping, laughing, directing traffic*). For these actions, participants observed a stick figure performing an action without any verbal label provided and were then instructed to 'imitate the movements of the action.' These stick figure actions were selected from the Carnegie Mellon Graphics (CMU) Lab Motion Capture Database available online (http://mocap.cs.cmu.edu), generated from actors whose motions were already pre-captured. PLDs were thus created using the above method for each participant, a sex-matched friend, and a sex-matched stranger. The stranger's action was randomly selected from one of three possible distractors for each sex (six total), pre-captured from actions of two of the experimenters and research assistants. The categorization of the action types, in addition to providing variability of the action goal, allowed us to further explore secondary analyses contrasting actions involving less motor familiarity due to copying someone else's motor plan (visual instruction) versus actions that involved more motor familiarity due to freely performing the action (verbal instruction).

Procedure

Behavioral Session

In the first session, participants' body movements were recorded using the Microsoft Kinect V2.0 and Kinect SDK in a quiet testing room. Participants were instructed to perform the actions in a rectangular space, in order to provide flexibility in how to perform the action, while remaining within recording distance. The Kinect was placed 1.5 m above the floor and 2.59 m away from the participant. Participants were instructed to naturalistically perform 12 actions as described above and recorded by our motion capture system. Participants signaled the start and stop of action performance by performing an outstretched T-Pose with their arms. Participant actions were then recorded and converted to point-light stimuli for use in the fMRI session.

Each of the 20 participants also brought a close friend of the same sex, who was also separately recorded with the same paradigm. None of the participants were informed about the study's purpose on self-recognition, but were informed that this study was about general visual action processing. We used the recordings of the close friend in the fMRI session to assess the impact of visual familiarity. After the recording session, participants completed a few attitudinal questionnaires including the Autism-Spectrum Quotient (AQ; Baron-Cohen et al., 2001), Schizotypal Personality Questionnaire (SPQ; Raine, 1991), and Vividness of Motor Imagery-2 (VMIQ-2; Roberts et al., 2008). These questionnaires were selected since they measure motor simulation ability (VMIQ-2) or disturbances in sensorimotor self-recognition (SPQ, AQ).

[Fig 1.tif]

fMRI session

After a delay period of two to three weeks (mean delay days = 18.55, *SD* = 2.87), participants returned for fMRI brain imaging in Session 2 (trial structure depicted in Figure 1). During brain imaging, participants passively observed a point-light display consisting of 25 joints. These joints included the head (head, neck, clavicle; 3 dots), arm (biceps, elbows, wrists; 6 dots), hands (fingers; 6 dots), stomach (1 dot), hips (3 dots), knees (2 dots), leg (shin, feet; 4 dots). Each point-light display either showed their own action (self), same-sex familiar friend, or same-sex stranger action for a five second duration. The same-sex stranger was selected at random (out of two options) between participants. After the stranger was selected, this stranger was consistently used for all actions involved in the experiment for this participant. Following the five second observation of the action, participants were prompted to identify on the next screen whether the action video shown was their own, friend, or stranger within a two second maximum response period. Participants responded with their right hand by pressing one of three keys, having the index finger on the first, the middle finger on the second, and the ring finger on the third key. One identity was assigned to each key, and identity-key mapping was counterbalanced across subjects. Participants' response was followed by jittered intertrial intervals (ITI) mean-centered at 5 seconds. There were four runs per participant, each consisting of 36 trials (12 trials per identity condition) in an event-related design. For each run, experimental conditions were pseudorandomized to reduce stimulus autocorrelation related to order and sequence effects as well as correlated noise, such as scanner drift. Response mapping of self/friend/stranger was randomized between participants to reduce effects of trial structure or motor preparation and planning demands. Duration of the experimental task during functional brain imaging was around 24 minutes. Total brain imaging duration lasted approximately 45 minutes.

Experimental Design and Statistical Analysis

MRI Acquisition

The Siemens 3-Tesla Prisma Fit scanner at the Staglin IMHRO Center for Cognitive Neuroscience was used for Magnetic resonance imaging, equipped with a 32-channel head coil. Structural data was acquired using a T1-weighted MPRAGE protocol (1.0 mm^3 resolution; repetition time = 2000 ms). Functional data was acquired utilizing T2*-weighted Gradient Recall Echo sequence. Scanning parameters for the main task included: repetition time = 700 ms, echo time = 33 ms, voxel size = 2.5 mm^3 voxels, field of view = 192 mm, flip angle = 70°. Four dummy scans were acquired and discarded before each scan to account for scanner stabilization. Participants viewed the stimuli presented on a projector through a mirror mounted on the head cover in the scanner. Participants underwent four runs of 36 trials each. Each run lasted approximately 360 seconds.

Imaging Analyses

Univariate Analysis

Statistical analyses were conducted using FEAT (FMRI Expert Analysis Tool) Version 6.00, part of FSL (FMRIB's Software Library, www.fmrib.ox.ac.uk/fsl) using the GLM approach. Individual functional scans were coregistered to the high resolution structural image using boundary-based registration (Greve and Fischl, 2009). Registration of the high-resolution structural scan to the Montreal Neurological Institute (MNI) template was implemented using FSL's FLIRT (Jenkinson 2001, 2002) with 12 parameter DOF affine transformation. The following pre-processing steps were applied: motion correction using MCFLIRT (Jenkinson 2002); slice-timing correction using Fourier-space time-series phase-shifting; non-brain tissue removal using BET (Smith 2002); spatial smoothing using a Gaussian kernel of FWHM 5mm; grand-mean scaling of the entire 4D dataset by a single multiplicative factor; high-pass temporal filtering (Gaussian-weighted leastsquares straight line fitting, with sigma=50.0s). Regressors were defined based on the onsets and durations of the three identities (self, friend, stranger) across all actions. Individual runs were aggregated into a mixed effects higher-level model using FLAME (FMRIB's Local Analysis of Mixed Effects) stage 1 and stage 2 (Beckmann et al., 2003; Woolrich, 2004; Woolrich 2008) for both within-session single subject variance and between-session group level variance. Significance testing on the statistical parametric maps was then assessed at the group level using two approaches in FSL: (1) *randomise* with threshold-free cluster enhancement (TFCE) and $p < .05$ FWE-corrected (Winkler et al., 2014; Smith & Nichols, 2009), TFCE-*p* threshold = .05 and (2) random-field (RFT) based thresholding at $Z > 3.1$, cluster corrected to a significance level of $p < .05$ (Worsley 2001). *Randomise* served as our main approach to significance testing given its more conservative, specific, and sensitive significance criteria (Smith & Nichols, 2009). All figures and tables generated from the parametric RFT analysis are reported in Extended Data 5-2, 5-4, 5-5. Conjunction analysis to localize self-specific activity was also implemented in FSL using the easythresh_conj script (easythresh_conj) on univariate activation maps for both *self* > *stranger* and *self* > *friend* contrasts (Nichols et al., 2005; Price & Friston, 1997). The conjunction specifically tested the "conjunction null hypothesis" as to whether both conditions showed significant functional activation ($Z > 3.1$, $p < .05$), which were later used as seed regions in the connectivity analyses.

Functional connectivity: Psychophysiological Interaction (PPI)

To identify a neural circuitry prioritized for self-processing, we implemented PPI (Friston et al., 1997) to assess task-specific changes in functional connectivity. PPI examines how the relationships between a seed region and voxels in other brain regions are modulated by the psychological state of the participant (task-dependent). The degree to which the seed regions and sink (other brain regions) vary as a function of the task, is measured by testing the significance of the β coefficient of the interaction computed between the experimental contrast vector and the sink region. As our analyses focused on identifying a self-action circuitry, we constrained our seeds to those determined by group-level functional activations in separate GLMs for the self (i.e., *self* > *stranger* or *self* > *friend* contrasts). We used a conjunction analysis implemented in FSL using the easythresh_conj script (easythresh_conj) on univariate activation maps for both *self* > *stranger* and *self* > *friend* contrasts. The seed region in the left IPL was generated from creating a sphere (8mm radius) around the peak functional activation for the conjunction of the self > stranger and self > friend contrasts (centered at peak center-of-gravity, x, y, z = -56, -44, 42). We initially focused on the IPL in the left hemisphere, since the TFCE thresholding only produced left hemispheric activity in the IPL. However, to more comprehensively investigate IPL involvement during self-processing, we also conducted PPI with the right hemisphere IPL seed. The seed regions were each defined in standard space and resampled to match 2.5mm isotropic voxel resolution. The resampled masks were then inversely transformed to native space, applied with nearest neighbor interpolation. Time courses in the seed region were extracted using fslmeants (https://fsl.fmrib.ox.ac.uk/fsl/fslwiki/Fslutils), which generated a vector of mean activity in the mask for each volume. This time course was then entered as the ROI time series regressor into the PPI GLM. Thus, the full GLM consisted of the interaction vector (PPI regressor), the main effects of the contrasts of interest (the psychological variables), and a vector representing the seed region time course (the physiological variable, Y regressor). At the group level, statistical parametric maps for the interaction term were thresholded ($Z > 2.3$, $p < .01$) to compute significance of the interaction term.

Representational Similarity Analysis

Whole-brain representational dissimilarity analysis (RDA) (Haxby et al., 2014; Krieskegorte et al., 2008) was implemented using the CoSMoMVPA toolbox (http://www.cosmomvpa.org/; Oosterhof et al., 2016) and custom MATLAB scripts (R2020a). Regressors were defined based on the onsets and durations of the three experimental conditions (self-actions, friend-actions, or stranger-actions) during the action observation period of the task. Using the Least-Squares Separate approach, beta-series parameter estimates (Rissman, Gazzaley, & D’Esposito, 2004; Mumford et al., 2012) were iteratively estimated per trial by modeling a regressor for the event of interest in the trial and a regressor for all other events within the run. Standard motion parameters were also included as regressors in each GLM. Preprocessing was identical to the univariate analysis, but no smoothing was applied. We generated multiple target representational dissimilarity matrices (RDM)s based on differences related to spatiotemporal movement distinctiveness (dynamic time warping), speed, acceleration, jerk, body structure consisting of limb segment length, and a theoretical RDM based on proprioceptive familiarity. To generate neural RDMs for each participant, we extracted 36 beta weights for each run, normalized each beta weight within run, computed the average for each of the 36 action targets across all runs, and then demeaned the data (i.e., subtraction of the grand mean of all averaged targets from each averaged target). All RDMs (behavioral, theoretical, and neural) were square, symmetric, and reflected the pairwise dissimilarity between each element in the matrix. Each RDM (proprioceptive familiarity, identity, movement distinctiveness, speed, acceleration, jerk, body structure) was either correlated separately with neural activity (standard RDA) or entered as input into a multiple regression RDA with other RDMs. The RDMs in the multiple regression analysis included a subset of the prior RDMs: proprioceptive familiarity and identity (self, friend, or stranger), and visual feature-based models related to movement distinctiveness (DTW), and speed. Each RDM was z-transformed prior to estimating the regression coefficients in the multiple regression analysis.

For the whole-brain searchlight RDA, each searchlight window was defined by a Gaussian sphere of 2-mm radius. Each spherical searchlight included every voxel in the brain, along with neighboring voxels within the window. The standard searchlight RDA was implemented through correlating the target RDM with neural RDM in each searchlight across the whole-brain. The correlations were then Fisher-*z* transformed and mapped to the center of each searchlight to create individual similarity maps in native space as inputs to the higher-level nonparametric analyses. For the multiple regression searchlight RDA, a multiple regression analysis was conducted in each searchlight across the whole-brain. For each participant in native space, the betas were mapped to the center of each searchlight to create individual similarity maps for each predictor as inputs to the higher-level non-parametric analyses. All individual maps were normalized to the MNI-152 template using FSL's FLIRT functionality (https://fsl.fmrib.ox.ac.uk/fsl/fslwiki/FLIRT) using trilinear interpolation for group-analysis. One-sample t-tests were computed at the group level, correcting for multiple comparisons using permutation-based threshold-free cluster enhancement with a corrected threshold of *p* < 0.01 (Smith and Nichols, 2009) with 10,000 Monte Carlo Simulations.

[Fig 2.tif]

Target Representational Dissimilarity Matrices:

Shown in Figure 2, we constructed the following representational dissimilarity matrices used as predictors for both standard and multiple regression representational dissimilarity analyses:

Movement Distinctiveness. The behavioral RDM for movement distinctiveness was generated using the dynamic time warping (DTW) algorithm to compare trajectory differences between a pair of actions. DTW measures the pairwise movement dissimilarity between action time series via an alignment procedure that accounts for variability in time series length or duration. DTW aims to find the lowest cost function (warping path) between pairwise action time series that stretches or shrinks the time series to reflect warped distances. Greater DTW values indicate greater movement dissimilarity between joint trajectories. A 36 x 36 RDM was created for each participant that computed the pairwise DTW dissimilarity between each of the 12 actions across each identity (self, friend, stranger). The following steps were implemented for Dynamic Time Warping (DTW) analysis in MATLAB R2020a:

(1) For each participant’s actions, 3D positions of each of the 25 joints were extracted using the BioMotion toolbox (van Boxtel & Lu, 2013).

(2) Each joint trajectory was centered to zero in order to remove the impact of global factors (e.g., global body displacements, limb length, etc.) on the similarity measures.

(3) The action DTW algorithm (Pham, Le, & Le, 2014) was implemented to search for a temporal warping function shared across all 25 joints.

(4) After deriving the optimal warping function, the analysis computed the frame-by-frame Euclidean distances of the temporally warped joint trajectories in actions performed by different actors.

(5) DTW distance was computed as the sum of the distances between all joint trajectories normalized by the number of frames of a target actor. This normalization step is required to account for the different durations across participants performing the same action.

(6) For each participant, the dissimilarity of the target participant performing an action from all other identities was captured by a mean DTW distance measure, computed by averaging across pairwise DTW distances between the target participant with the other actors (friend, stranger) in performing this action to construct the 36 x 36 representational dissimilarity matrix (RDM).

Speed, Acceleration, and Jerk Differences. To measure the contribution of movement speed to self-recognition, we calculated a speed distinctiveness value for every participant's individual action in MATLAB R2020a. For each action, we computed the average 3D positional displacement across all frames and all 25 joints (using the first-order derivative of position) extracted from Biomotion Toolbox (Van Boxtel & Lu, 2013). We then computed the average pairwise Euclidean distance to all other identities and actions as a measure of speed distinctiveness to construct the 36 x 36 RDM. Acceleration and jerk were identically computed, though taking the first and second derivative of speed respectively.

Body Structure (postural limb length). The body structure RDA was computed based on the limb length of each of the 24 limbs (for 25 joints) of the PLD. Limb length was computed using the 3D Euclidean distance between pairs of joints that made up each limb in the PLD. Pairwise absolute value dissimilarities were then calculated across participants for each limb and averaged together across all limbs to comprise the 36 x 36 target RDM.

Motor familiarity. We computed a simple theoretical RDM based on the theorized motor familiarity between each of the identities. This was based on common coding theory (Prinz, 1997), which posits a common representational platform and shared overlap between visual and motor codes. Thus, identity for the self was coded as 0 (most familiarity due to prior motor experience; least dissimilarity). We coded friend as 0.6 to capture the low-medium level of familiarity, since participants had a high degree of visual familiarity with the friends' actions, translating to a small degree of motor familiarity. Note that the specific value of 0.6 was not critical, as the main findings (as described in the results section) remained for a range of possible values. Since common coding theory posits shared or overlapping visual and motor codes, repeated visual exposure to friends' actions could establish partial motor simulation, where repeated observation of common movements of familiar friends activates motor circuits even without direct execution of those actions (Rizzolatti and Craighero, 2004; Gallese 2006). This would account for stronger neural encoding seen for friends' actions compared to strangers. Hence, stranger was coded as 1 for all actions (no familiarity; most dissimilarity). Within self-identity, we further weighted the actions by their motor familiarity. Specifically, actions that were more motorically familiar to participants due to freely performing the action and self-generating the motor plan (i.e., via verbal instruction) were coded as most similar (0). Actions that involved copying someone else's motor plan (i.e., imitated via visual instruction) were coded as less familiar (.3). All other identities (friend, stranger) were computed equally similar across actions (friend coded as 0.6, stranger coded as 1). Thus, dissimilarity was computed between identities and weighted by motor familiarity to comprise the 36 x 36 theoretical RDM.

Identity: Self (motor familiarity), Friend (visual familiarity), or Stranger. We also computed theoretical RDMs specific to identity for either self actions, friend actions, or stranger actions. For each identity RDM, the identity of interest (e.g., self) was coded as 0 (most similar), while the other two identities (e.g., friend, stranger) were coded equally as dissimilar (1). Dissimilarity was only computed between identities (and not individual actions) to comprise 36 x 36 theoretical RDMs for each identity (self RDM, friend RDM, or stranger RDM).

Results

Identity recognition from sparse actions

First, we examined whether self-recognition was possible in visually sparse point-light displays. We found that participants could discriminate all identities (self, friend, stranger) significantly above chance (.33), self: *M* = .563, *SD* = .180, *t*(19) = 5.789, *p* < .001, cohen's *d* = 1.29; friend: *M* = .483, *SD* = .182, *t*(19) = 3.754, *p* = .001, *d* = .839; stranger: *M* = .5052, *SD* = .172, *t*(19) = 4.554, *p* < .001, *d* = 1.01 (Figure 3).

[Fig 3.tif]

Recognition of self-generated actions (*M* = .563, *SD* = .180) was significantly higher than friends' actions (*M*= .483, *SD* = .182), *t*(19) = 2.673, p_{adj} = .049, *d* = .598, but not significantly higher than correctly identifying strangers' actions (*M* = .505, *SD* = .172), *t*(19) = 1.353, p_{adj} =

.192. Self-recognition accuracy was also modulated by motor planning, revealed by a significant interaction effect between action type and identity $F(2,19) = 7.546$, $p = .002$, $\eta_p^2 = .284$. Specifically, actions that were generated by one's own motor plan (i.e., verbally instructed; $M = .615$, $SD = .198$) were better recognized relative to actions that were performed by copying someone else's motor plan (visually instructed, $M = .513$, $SD = .189$), $t(19) = 3.170$, $p_{adj} = .049$, $d = .709$. This behavioral result supports the hypothesis that motor processes are involved in self-recognition. Motor planning did not modulate recognition accuracy for any of the other identities, friends $t(19) = .340$, $p = .999$, nor strangers, $t(19) = -2.195$, $p = .285$. All post-hoc comparisons were corrected using Tukey's HSD.

As shown in the top panel of Figure 3, self-recognition was greatest for the stretch action ($M = .788$, $SD = .412$) and lowest for digging ($M = .375$, $SD = .487$). Across all actions, no relationships were found between self-recognition accuracy and distinctiveness related to speed ($p = .747$), acceleration ($p = .380$), postural length ($p = .410$), or movement dissimilarity ($p = .174$). These results confirm that action identity could be distinguished in the sparse visual displays, with an advantage for actions generated with one's own motor plan.

Action Observation Network is recruited for identity recognition

Our main goal was to examine the neural mechanisms underlying self-recognition from whole-body movements. To do so, we first compared neural activity for each identity (*self, friend, stranger*) relative to baseline. We found bilateral recruitment of the action observation network for all identities (overlayed in MNI space *Fig 4*). The activity spanned regions classically found in visual neuroscience, including the posterior superior temporal sulcus (pSTS) (right: $x,y,z = 56, 42, 10$, left: $x,y,z = -52, -50, 10$) and lateral occipital cortices, including extrastriate body area (EBA) (right $x,y,z = 44, -60, 10$; left $x,y,z, =-51, -69, 10$),$^+$ as well as regions with motor properties also described in the action observation literature (Rizzolatti & Craighero, 2004; Bonini et al., 2022), including the bilateral supplementary motor areas (right *x,y,z* = 12, 6, 56; left *x,y,z* = 4, -8, 52), premotor cortices (right *x,y,z* = 39,1,53*;* Left *x, y, z* = -45, 2, 50), inferior frontal gyri (IFG) (right *x,y,z* = 50, 15, 10; left *x,y,z* = -55, 16, 10), and inferior parietal lobules (IPL) (right *x,y,z* = 50, -40, 14; left *x,y,z* = -56, -44, 11).

[Fig 4.tif]

A frontoparietal network for self-action processing

Though visual and motor systems were involved during action observation of all identities, we expected greater activity in motor regions when participants observed their own actions, since self-generated actions are privileged by prior motor experience. According to common coding theory, vision and proprioception share a degree of functional equivalence, such that action recognition is facilitated by a matching process between these modalities (Prinz 1997; Hommel et al., 2001).

Since visual and proprioceptive codes are most closely matched when observing our own actions relative to observing actions of others, self-recognition should be facilitated in brain regions with motor properties that are also active during action observation (e.g., Knoblich and Flach, 2004; Limanowski and Blankenburg, 2016; Abdulkarim et al., 2023). Indeed, both self contrasts of interest (*self* > *stranger* and *self* > *friend*) uniquely evoked greater activity in frontoparietal regions with these properties. For *self* > *stranger*, activity was localized to the left posterior supramarginal gyrus (peak *x, y, z* = -62, -48, 28) into the angular gyrus, as well as the left insular cortex and the inferior frontal gyrus, pars opercularis (*x,y,z* = -42, 10, -8) *(*Figure 5). A few small clusters in the anterior cingulate cortex (ACC) (*x,y,z* = -2, 20, 18; *x,y,z* = 4, 14, 28) and one small cluster in the right insular cortex (*x,y,z* = 40, 10 ,-2) were also observed. *Self* > *friend* similarly recruited the left posterior SMG of the IPL (*x,y,z* = -54, -50, 30), spanning the angular gyrus (Figure 5, right panel). For *friend* > *stranger and stranger* > *friend,* FSL's *randomise* approach did not yield significant activity. All peak clusters from the analyses are reported in the Extended Data Tables 5-1, 5-2, and 5-3.

[Figure 5.tif]

Coactivation in these regions does not necessarily implicate a network for self-processing. Thus, we further measured network-related activity during self-processing using task-based functional connectivity (PPI; Friston et al., 1997). The bilateral IPL (peak sphere from the group-level conjunction maps for self-processing: left: *x, y, z* = -56, -44, 42; right: 54, -38, 40) was set as seed regions in separate PPIs, due to the important role of the IPL in motor simulation and hub status in action processing.

We found very similar results across both hemispheric seeds. For both seed regions, we observed strengthened frontoparietal and parieto-visual connectivity for the self-processing contrasts (*self* > *stranger* and *self* > *friend*). The left IPL seed for *self* > *stranger* showed the greatest peak connectivity between parieto-visual regions: the right lateral occipital cortex (*x, y, z* = 54 -50, -2), and the left occipito-temporal fusiform area (*x, y, z* = -52, -70, -12). We also found strengthened frontoparietal connectivity, specifically with the bilateral inferior frontal cortices (left *x, y, z* = -54, 16, 30; right *x, y, z* = 46, 18, 20), as well as bilateral intraparietal sulcus spanning the somatomotor cortex (left *x, y, z* = 26, -50, 44, right *x, y, z* = 32, -36, 44) (Figure 6). For the right IPL seed, we found similar connectivity patterns to the left. For *self* > *friend* with the right IPL seed, we found the greatest frontoparietal functional connectivity, between the right IPL and the bilateral inferior frontal cortex (*x,y,z* =-36, 30, 34), extending from the middle frontal gyrus to the IFG pars opercularis, and spanning the primary motor cortex and premotor cortex. Additional activity was found in the right pre-SMA (*x,y,z* = 4,12,58) as well as bilateral occipotemporal regions, with peaks in the right occipital-temporal cortex (*x,y,z* = 46, -56, -2) and left superior temporal sulcus (*x,y,z* = -62, -50, 8). For *self* > *stranger,* we observed strengthened parieto-occipitotemporal activity, with peaks in the left lateral occipito-temporal cortex (*x,y,z* = -46, -68, 12), and right fusiform area (*x,y,z* = 42, -40, -20). Additionally, we found strengthened connectivity with the frontal lobe, with peaks in the bilateral inferior frontal cortex, spanning the premotor and primary motor regions. No activity was found for *friend* > *stranger.* All activity maps were cluster corrected at *Z* > 2.3, *p* < .01.

[Figure 6.tif]

Table 1. PPI results with bilateral IPL seeds

Region	Contrast	Hemisphere	Area	MNI (*x,y,z*)	Max Z	Cluster Size	*p*
Left IPL							
	Self > Stranger	Right	Fusiform Area	54, -50, -2	4.09	2265	<.0001
		Left	Fusiform Area	-52, -70, -12	4.09	1660	<.0001
		Right	IFC	46, 18, 20	4.05	1537	<.0001
		Left	IFC	-54, 16, 30	4.01	1932	<.0001
			IPS	32, -36, 44	3.56	807	<.0001
			IPS	-26, -50, 44	3.74	1142	<.0001
	Self > Friend	Right	IFC	50, 14, 44	3.83	629	<.0001
		Left	IFC	-50, 26, 28	3.69	1216	<.0001
		Right	Fusiform Area	42, -60, -10	3.93	1154	<.0001
		Left	Fusiform Area	-48, -50, -20	3.57	401	.003
		Left	Middle Temporal	-60, -50, 4	4.02	609	<.0001
Right IPL							
	Self > Stranger	Left	LOC	-46, -68, 12	3.91	1418	<.0001
		Right	Fusiform Area	42, -40, -20	3.57	1248	<.0001
		Right	IFC	38, 30, 20	3.58	885	<.0001
		Left	IFC	-44, 12, 28	3.63	703	<.0001

Left	STS	-62, -50, 8	3.57	781	<.0001
Right	Pre-SMA	4,12, 48	3.78	576	<.0001
Right	OTC	46, -56, -2	3.32	482	.00031
Left	MFG	-36, 30, 34	3.43	415	.00111

Evaluating a visuomotor representational space for self-processing

Based on the strengthened frontoparietal connectivity for self-processing, the analysis below focused on underlying representational structure. Specifically, we examined the extent to which self-recognition relied on factors that resembled motor familiarity, while accounting for visual signatures of the actions across the whole-brain using multiple regression RDA. We opted for whole-brain analyses since frontoparietal regions often comprise multiple brain networks (e.g., action observation network, central executive network), and since additional regions associated with motor functions also encode self-processing. If self-recognition relies on motor mechanisms, then encoding patterns may further span other regions associated with motor properties, such as the somatomotor cortex. Thereafter, we conducted four multiple regression RDAs for the following predictors of interest: (1) motor familiarity and (2) for each identity: (2a) self, (2b) friend, or (2c) stranger in separate regression models, accounting for visual features related to speed or movement distinctiveness.

Multiple Regression Motor Familiarity RDA: somatomotor cortex and occipitotemporal regions

The motor familiarity representational dissimilarity matrix was computed based on the theorized motor familiarity between each of the identities (self as most motorically familiar, friend as medium, and stranger as least). Within self-identity, we further weighted the actions by their degree of motor familiarity. Actions that were most motorically familiar to participants due to self-generating the motor plan were coded as most similar. Actions that involved copying someone else’s motor plan (i.e., imitated via visual instruction) were coded as less familiar.

Shown in Figure 7, we found robust encoding in the somatomotor, frontoparietal, and lateral-occipital cortices. Specifically, the motor familiarity multiple regression RDA (accounting for differences in speed and movement distinctiveness) revealed the largest pattern of encoding in the bilateral primary motor cortex (M1), spanning the primary somatosensory cortex (S1), and showed stronger representation in the left hemisphere (left peak *x,y,z* = -46, -22, 50) than right (right peak *x,y,z* = 52, 1, 34). Activity patterns were also found in fronto-parietal regions, including inferior parietal (right peak *x,y,z*: 54, -36, 36, left peak *x,y,z*: 46, -66, 34), and a large cluster spanning the anterior cingulate, mid-superior frontal areas, and supplementary motor areas (right peak *x,y,z* = 11, 50, 17; left peak *x,y,z* = -18, 3, 41). Activity patterns were also observed in the occipital and lateral-occipital regions, extending into the bilateral lingual gyrus, precuneus, cuneus (right peak *x,y,z* = 22, -61, -2). These results together reveal a gradation of encoding in motor-related regions using identity-based motor familiarity. Specifically, motor-related brain regions were most strongly encoded when viewing self-generated actions, followed by friend, and followed by stranger. An exhaustive table of all activity patterns is reported in Extended Data Table 7-1.

[Fig 7.tif]

Multiple Regression Identity RDAs: stronger representation in somatomotor cortex and mPFC

We then measured whether the representational encoding found in these regions was specialized for self-identity. We compared activity patterns generated from multiple regression

RDAs that specified self-actions as the predictor of interest, as compared to multiple regression RDAs for each other identity (friend, or stranger).

The self-identity RDA generated the largest activity patterns in the bilateral somatomotor regions, with its peak in the left hemisphere (left peak x,y,z = -30,-23,57) and visually identified in the right hemisphere (right peak x,y,z = 40, -12, 50) (Figure 8). We also found large activity patterns in frontoparietal regions, spanning the IPL (left peak x,y,z = -37,-64,40; right peak x,y,z = 60,-36,27), supplementary motor area (left peak x,y,z = -8,-7,58, right peak x,y,z = 11,15,58), and lateral to medial-prefrontal cortices (peak x,y,z = 46,50,4) for the self-identity multiple regression RDA. These results suggest that the somatomotor and frontoparietal regions–associated with motor simulation–primarily encoded self-actions relative to actions of others. Further, the strength of encoding in the somatomotor and frontoparietal cortices systematically degraded as a function of identity. Specifically, the friend RDA produced less encoding, and the stranger RDA produced no significant encoding in these regions. Activity patterns were also most visually distributed for the self, followed by friend, and followed by stranger (examined at a reduced threshold, *p*<.05).

Additional activity patterns unique to self-identity were also found in bilateral parahippocampal gyri (left peak *x,y,z*= -16,-13,-20, right peak *x,y,z*= 32,-28,-4), with much smaller activity patterns found in the left occipital pole (left peak *x,y,z*= -23,-98,-14), bilateral temporal pole (right peak *x,y,z*= 46,4,-33, left peak *x,y,z*= -32,-39,16), thalamus (peak *x,y,z* = 14,-22,18), and precuneus (peak *x,y,z*= 8,-38,6). For the friend RDA, the activity patterns were noticeably sparser and largely overlapped with self-identity, but mostly constrained to the cortical midline. These regions spanned the precentral gyri, SMA, IPL, insula (peak x,y,z = -46, -30, 23), the left calcarine and occipitotemporal regions (peak *x,y,z* =-16, -61, 16), and thalamus (peak *x,y,z* =-8, 34, -0). For the stranger RDA, only sparse activity patterns were found in visual regions: right middle temporal gyrus and occipitotemporal cortex (peak *x,y,z* = 62, -47, 6) at a reduced threshold (Z > 1.96). See Extended Data (Tables 8-1, 8-2, 8-3) for an exhaustive report of all clusters from all RDAs, visually depicted in Figure 8.

[Fig 8.tif]

Table 2. Number of voxels in regions of interest for each main identity RDA. Table depicts a parametric degradation in activity pattern encoding in somatomotor and frontoparietal regions as a function of person-identity.

Area		Self	Friend	Stranger
Somatomotor		5675	1843	0
Frontoparietal				
	IPL	2383	913	2
	SPL	1192	481	0
	IFG	860	322	0
	INS	740	198	0

Abbreviations: IPL (Inferior Parietal Lobule); SPL (Superior Parietal Lobule); IFG (Inferior Frontal Gyrus); IS (Insular Cortex). Number of voxels calculated within region of interest (ROI) masks generated from Harvard-Oxford Cortical Atlas for each identity RDA map (self, friend: *p*s < 0.01, and stranger: $p < 0.05$). Somatomotor mask was generated by combining precentral and postcentral gyri masks. IPL mask determined by the combination of parietal operculum, angular gyri, and supramarginal gyri (anterior and posterior) masks, subtracting occipito-temporal overlap (medial temporal gyri and lateral occipital cortices). IFG mask determined by combination of IFG pars triangularis and IFG pars opercularis masks. Insula mask determined by subtracting IFG mask from Insula ROI.

Finally, to account for any effect of motor planning of the button responses producing the large motor cluster in the left-hemisphere for the self-RDA, we conducted an additional RDA for self-identity that included the timing of the motor responses as a covariate in the multiple regression analysis. The results maintained the original findings of the self-RDA. Specifically, the largest cluster from the RDA was observed in the left somatomotor cortex (left peak *x,y,z* =-42, -20, 46), and preserved the main findings. See Extended Data (Table 9-1) for an exhaustive report of all clusters from the RDA, visually depicted in Figure 9.

[Figure 9.tif]

Combined with results from the motor familiarity RDA, these findings lend support to motor simulation accounts. Self-processing, due to its high degree of motor familiarity, would be expected to have the strongest degree of motor simulation during action observation, reflected by the largest activity patterns in motor-related regions, followed by friend, then stranger. This aligns with prevalent accounts suggesting that action observation of others involves an internal simulation of the action onto our own motor systems (e.g., Rizzolatti & Craighero, 2004; Iacoboni, 2008).

Discussion

Our study investigated the neural correlates for self-recognition of our whole-body movements. On functional brain imaging data, we report that merely observing our whole bodies in motion evokes greater activity in neural systems traditionally construed as having motor functions, in comparison to observing the actions of others.

While boundaries between visual and motor functions have been increasingly blurred over the last few decades of systems neuroscience research, traditionally frontoparietal areas are mostly conceived as having motor functions, whereas occipito-temporal areas are typically construed as involved in visual processing. Here, we found that both areas were involved in action observation of all identities. However, unique to self-action observation, we observed greater activity and functional connectivity of frontoparietal regions (left inferior parietal lobule; IPL and inferior frontal cortex; IFC), functionally connected to occipito-temporal regions. Note that significance for all univariate subtraction contrasts was assessed using non-parametric threshold-free cluster enhancement (TFCE), as TFCE has been shown to be more sensitive yet less prone to false positives in the literature (Smith & Nichols, 2009). This resulted in left-lateralized activity for self-processing. However, bilateral involvement of these regions was clearly observed when using FSL's standard RFT cluster correction ($Z > 3.1$, $p < .05$) as well as in our multivariate analyses. To avoid false positives, we interpret the non-parametric results, but do not make strong claims on observed laterality.

Action simulation accounts posit a central role of the motor system during action observation (Gallese & Goldman, 1998; Rizzolatti & Sinigaglia, 2010). The degree of motor experience with actions is thought to parametrically modulate activity in these frontoparietal and motor regions during action observation (even across modalities, e.g., Kaplan et al., 2008; Kirsch and Cross, 2015; Blakemore & Frith, 2003). Since self-generated actions benefit from prior motor experience, action simulation could be one candidate mechanism for the increased activity and connectivity in these regions. However, these regions, notably frontoparietal, also support functions beyond action simulation, including working memory (Baddeley, 2003), cognitive control (Corbetta & Shulman, 2002), and multisensory integration (Macaluso & Driver, 2005). While we are unaware of any direct links between cognitive control and self-recognition on a visual perception task—multisensory integration, particularly in the IPL, could be an important mechanism to facilitate self-action recognition by combining visual and proprioceptive information. Similarly, working memory could facilitate retention of the action in order to differentiate identity, implicating the intraparietal sulcus and numerous occipitotemporal regions (Woźniak et al., 2022).

It is important to note that merely observing actions may not veridically engage the same cognitive and neural resources associated with action simulation. For instance, while action observation can engage sensorimotor areas, it may not trigger the same internal model mechanisms that would predict somatosensory attenuation during action production, as expected in action simulation accounts (Kilteni et al., 2021). Conversely, other processes such as motor imagery, can engage these mechanisms (Kilteni et al., 2018). Hence, we do not make strong claims on positing the functional mechanism associated with these areas, but highlight action simulation as one possible candidate.

Strengthened connectivity was also observed between the bilateral IPL and the inferior frontal cortex (IFC) anterior to the premotor cortex, during self-action recognition. Action simulation accounts often implicate both the IFC and IPL, two anatomically and functionally connected areas. Other proposals suggest that anterior parcellations of the IFC might be locally involved in abstracted aspects of action understanding, such as goal selection, intention inference, and semantic understanding (e.g., Liakakis et al., 2011). During self-action recognition, the IFC (including its more anterior portions) could support the integration of action observation with higher-order cognitive processes. Information flow may originate from strengthened parieto-occipitotemporal functional connectivity during action processing, then passed onto the IFC (in both anterior and posterior IFG in our data) for more conceptual action understanding.

Our results also highlight the role of parieto-occipitotemporal regions in action observation. These regions may distinguish fine-grained visual features that facilitate discrimination between identities. Together with the IPL and the IFC (e.g., Kilner, 2011), this set of areas may form an expanded action observation network for self-recognition. That is, occipital-temporal regions first decode coarse visual identity based on low and mid-level action features (including for person perception in the superior temporal sulcus, Isik et al., 2017), while frontoparietal regions may process self-actions at a deeper motoric, proprioceptive, and conceptual level (e.g., Rizzolatti et al., 2014; Rizzolatti & Craighero, 2004).

In addition to frontoparietal and occipitotemporal regions engaged during self-action observation, the multivariate results revealed largest activity patterns in bilateral somatomotor regions. Activity in these regions for both the motor familiarity and self-identity representational (dis)similarity analyses (RSA)s spanned the primary motor, primary somatosensory, supplementary motor areas, and the premotor cortices. Further, the strength of encoding in the somatomotor and frontoparietal cortices systematically degraded as a function of identity. These regions most strongly encoded self-identity, moderately encoded friend-identity, and did not encode stranger-identity, which instead revealed activity patterns in primarily occipito-temporal regions. The relatively parametric degradation of somatomotor and frontoparietal encoding as a function of person identity lends further support to action simulation accounts.

While neural activity in these frontoparietal and somatomotor regions is often implicated in motor production (e.g., Muir and Lemon, 1983) as well as control, attention, and working memory processes as noted earlier, these regions are often functionally implicated in tasks involving action simulation, including action observation (Gallese & Goldman, 1998; Keysers and Gazzola, 2010), motor imagery (Schnitzler et al., 1997; Ehrsson et al., 2003; Porro et al., 2000; Pilgramm et al., 2016; Pfurtscheller & Neuper, 1997), action prediction (Lamm, Fischer & Decety, 2007; Blakemore and Frith, 2003), motor memory (Romo et al., 2012), and motor planning (Gale et al., 2021). Moreover, coactivation in both premotor and posterior parietal areas appears to depend on the match between motor and visual information that facilitates one’s sense of body ownership (e.g., Abdulkarim et al., 2023). The greater match between common visual and proprioceptive codes may provide the increased sense of bodily awareness needed to facilitate self-recognition. This is reflected by the greater signal encoding in these regions for the self, which degraded by visuomotor person familiarity (i.e., less for friend, none for stranger).

The RSA results also revealed that the neural encoding was most distributed for self-identity, followed by friend, and least for stranger, where it was primarily localized to occipito-temporal regions. A substantial body of research suggests that self-processing generally engages systems-wide and distributed activity compared to processing other identities (e.g., Molnar-Szakacs & Uddin, 2013; Turk et al., 2003; Yeshurun et al., 2021). Indeed, at the network-level, self-processing involves strong interactions between both low-level feature-based processing, and higher-level conceptual processing, facilitating a sense of identity due to the wealth of information we have stored about our own identities (Molnar-Szakacs & Uddin, 2013).

Results from the self-identity RSA also revealed distributed encoding patterns in other regions (see Extended Data Table 8-1). The activity patterns spanned regions traditionally associated with mentalizing (Frith & Frith, 2006) and higher-order reflective and conceptual self- and other-processing, including the bilateral posterior cingulate cortex, medial (and lateral) prefrontal cortex, bilateral hippocampus, and the precuneus. These regions not only engage during mentalizing for others, but also for conceptual mentalizing about oneself (Lombardo et al., 2010; Qin and Northoff, 2011), and conscious awareness of oneself (e.g., Tacikowski et al., 2017). Well-known action frameworks (e.g., Keysers and Gazzola, 2007) characterize a degree of dynamic connectivity between simulative motor representations and abstracted, self-reflective judgments. It is possible that these regions may store action representations in memory, or motor schemas, which are later accessed as a comparison to the visual consequence during action observation (Schmidt, 1975; Arbib 1981; Arbib, 1992). That is, rather than identifying one's body based solely on visual cues that we generally lack access to in daily life, we may access stored proprioceptive schemas at a more abstract level of processing (i.e., "remembered selves"; Neisser, 1988) that interact with action observation to facilitate the visuo-proprioceptive match needed for self-recognition.

Finally, a cluster of activity in the anterior cingulate cortex (ACC) was also observed in the RSA as well as a small cluster during the univariate task contrast of *self* > *stranger* actions. While ACC engagement may be due to multiple reasons given the many functional processes it has been associated with, a key account of ACC function is related to cognitive conflict (Braver et al., 2001). Prior research has shown that the ACC is involved in discriminating one's own touch from an external touch, with the activity linked to the conflict between expected and actual sensorimotor feedback (Blakemore et al 1998; Kilteni et al 2024; Stetson et al 2006). There may be a similar conflict mechanism here when participants merely view their own and other people's actions. The brain has well-established representations of self-generated actions, and viewing these actions might generate conflict between the internal sensorimotor expectations and the stimulus-driven visual feedback during action observation. This conflict should be less pronounced, or even absent when viewing others' actions, since the internal sensorimotor predictions for others' actions are less accessible.

In summary, our three main analyses— univariate, functional connectivity, and RSA— converge on a cortical ensemble of visuomotor regions, spanning frontoparietal, somatomotor, and occipito-temporal areas, that seem prioritized for self-recognition of whole-body actions. These regions, notably frontoparietal and somatomotor cortices, are often linked to simulative motor functions during action observation, which may provide a functional explanation for the increased motor-related activity we observed. Our findings together reveal an important contribution of motoric indices to human self-awareness, helping to facilitate the basic differentiation between ourselves and others.

Acknowledgements

We thank Sophia Baia and Kelly Xue for assistance with data collection and stimuli creation, and Elinor Yeo, Jolie Wu, Kelly Nola, Nicolas Jeong, Danya Elghebagy, David Lipkin, Shahan McGahee for assistance with stimuli creation. We thank Jeff Chiang, Burcu Ürgen, and Giuseppe Marrazzo for helpful advice on the analyses. We thank Lisa Aziz-Zadeh and Sofronia Ringold for helpful feedback on an earlier draft of this manuscript. This project was supported by National Science Foundation BCS- 2142269 to H.L., UCLA faculty research grant to H.L., Tiny Blue Dot Foundation grant to M.M.M., and APA Dissertation Award to A.K. Preliminary versions of this project were presented at the Virtual Society for Neuroscience (2020), V-Vision Sciences Society (2020), Society for Neuroscience (2022), and Association for Scientific Study of Consciousness (2023).

Data Availability: All analysis scripts, behavioral data, and results from the imaging analyses can be downloaded from our GitHub repository: https://github.com/akilakada/self-fmri. Raw nifti data can be shared upon request to the corresponding author and subject to the UCLA Institutional Review Board Guidelines.

References

Abdulkarim, Z., Guterstam, A., Hayatou, Z., & Ehrsson, H. H. (2023). Neural substrates of body ownership and agency during voluntary movement. Journal of Neuroscience, 43(13), 2362-2380.

Apps, Matthew AJ, and Manos Tsakiris. "The free-energy self: a predictive coding account of self-recognition." Neuroscience & Biobehavioral Reviews 41 (2014): 85-97.

Arbib, M. A. (1981). Perceptual structures and distributed motor control. In Handbook of physiology, section I: the nervous system, vol. 2: motor control (ed. V. B. Brooks), pp. 1449–80. Williams and Wilkins, Baltimore

Arbib, M. A. (1992). Schema theory. The encyclopedia of artificial intelligence, 2, 1427-1443.

Aron AR, Fletcher PC, Bullmore ET, Sahakian BJ, Robbins TW (2003) Stopsignal inhibition disrupted by damage to right inferior frontal gyrus in humans. Nat Neurosci 6:115–116.

Asakage, S., & Nakano, T. (2023). The salience network is activated during self-recognition from both first-person and third-person perspectives. Human Brain Mapping, 44(2), 559-570.

Astafiev, S. V., Stanley, C. M., Shulman, G. L., & Corbetta, M. (2004). Extrastriate body area in human occipital cortex responds to the performance of motor actions. Nature neuroscience, 7(5), 542-548.

Atkinson, A. P., Dittrich, W. H., Gemmell, A. J., & Young, A. W. (2004). Emotion perception from dynamic and static body expressions in point-light and full-light displays. Perception, 33(6), 717-746.

Baddeley, A. (2003). Working memory: looking back and looking forward. *Nature Reviews Neuroscience, 4*(10), 829-839.

Baron-Cohen, S., Wheelwright, S., Skinner, R., Martin, J., & Clubley, E. (2001). The autismspectrum quotient (AQ): evidence from Asperger syndrome/high-functioning autism, males and females, scientists and mathematicians. [erratum appears in J Autism Dev Disord 2001 Dec;31(6):603]. Journal of Autism & Developmental Disorders.

Beckmann, C. F., Jenkinson, M., & Smith, S. M. (2003). General multilevel linear modeling for group analysis in FMRI. Neuroimage, 20(2), 1052-1063.

Beardsworth, T., & Buckner, T. (1981). The ability to recognize oneself from a video recording of one's movements without seeing one's body. Bulletin of the Psychonomic Society, 18(1), 19-22.

Benjamini, Y., & Yekutieli, D. (2001). The control of the false discovery rate in multiple testing under dependency. Annals of statistics, 1165-1188.

Berlucchi, G., & Aglioti, S. M. (2010). The body in the brain revisited. Experimental brain research, 200(1), 25-35.

Blakemore, S. J., & Frith, C. (2003). Disorders of self-monitoring and the symptoms of schizophrenia. *The self in neuroscience and psychiatry*, 407-424.

Blakemore, S. J., Frith, C. D., & Wolpert, D. M. (1999). Spatio-temporal prediction modulates the perception of self-produced stimuli. *Journal of cognitive neuroscience*, *11*(5), 551-559.

Blakemore SJ, Wolpert DM, Frith CD. Central cancellation of self-produced tickle sensation. Nat Neurosci. 1998 Nov;1(7):635-40. doi: 10.1038/2870. PMID: 10196573.

Blanke, O. (2012). Multisensory brain mechanisms of bodily self-consciousness. Nature Reviews Neuroscience, 13(8), 556-571.

Blanke, O., Slater, M., & Serino, A. (2015). Behavioral, neural, and computational principles of bodily self-consciousness. Neuron, 88(1), 145-166.

Bischoff, M., Zentgraf, K., Lorey, B., Pilgramm, S., Balser, N., Baumgartner, E., ... & Munzert, J. (2012). Motor familiarity: Brain activation when watching kinematic displays of one's own movements. Neuropsychologia, 50(8), 2085-2092.

Bracci S, Caramazza A, Peelen MV (2015) Representational similarity of body parts in human occipitotemporal cortex. J Neurosci 35: 12977–12985. CrossRef Medline

Braver, T. S., Barch, D. M., Gray, J. R., Molfese, D. L., & Snyder, A. (2001). Anterior cingulate cortex and response conflict: effects of frequency, inhibition and errors. Cerebral cortex, 11(9), 825-836.

Bréchet, L., Grivaz, P., Gauthier, B., & Blanke, O. (2018). Common recruitment of angular gyrus in episodic autobiographical memory and bodily self-consciousness. Frontiers in behavioral neuroscience, 270.

Brady N, Campbell M, Flaherty M (2004) My left brain and me: a dissociation in the perception of self and others. Neuropsychologia 42:1156–1161.

Burling, J. M., Kadambi, A., Safari, T., & Lu, H. (2019). The impact of autistic traits on selfrecognition of body movements. Frontiers in psychology, 9, 2687.

Calvo-Merino, B., Grèzes, J., Glaser, D. E., Passingham, R. E., & Haggard, P. (2006). Seeing or doing? Influence of visual and motor familiarity in action observation. Current biology, 16(19), 1905-1910.

Candidi, M., Stienen, B. M., Aglioti, S. M., & de Gelder, B. (2011). Event-related repetitive transcranial magnetic stimulation of posterior superior temporal sulcus improves the detection of threatening postural changes in human bodies. Journal of Neuroscience, 31(48), 17547-17554.

Chang, D. H., Troje, N. F., Ikegaya, Y., Fujita, I., & Ban, H. (2021). Spatiotemporal dynamics of responses to biological motion in the human brain. Cortex, 136, 124-139.s

Cisler, J. M., Bush, K., & Steele, J. S. (2014). A comparison of statistical methods for detecting context-modulated functional connectivity in fMRI. *Neuroimage*, *84*, 1042-1052.

Conson, M., Aromino, A. R., & Trojano, L. (2010). Whose hand is this? Handedness and visual perspective modulate self/other discrimination. Experimental Brain Research, 206(4), 449-453.

Corbetta, M., & Shulman, G. L. (2002). Control of goal-directed and stimulus-driven attention in the brain. *Nature Reviews Neuroscience, 3*(3), 201-215.

Coste, A., Bardy, B. G., Janaqi, S., Słowiński, P., Tsaneva-Atanasova, K., Goupil, J. L., & Marin, L. (2021). Decoding identity from motion: how motor similarities colour our perception of self and others. Psychological research, 85(2), 509-519.

David, N., Cohen, M. X., Newen, A., Bewernick, B. H., Shah, N. J., Fink, G. R., et al. (2007). The extrastriate cortex distinguishes between the consequences of one's own and others' behavior.Neuroimage, 36, 1004e1014.

Darda, K. M., & Ramsey, R. (2019). The inhibition of automatic imitation: A meta-analysis and synthesis of fMRI studies. NeuroImage, 197, 320-329.

De Bellis, F., Trojano, L., Errico, D., Grossi, D., & Conson, M. (2017). Whose hand is this? Differential responses of right and left extrastriate body areas to visual images of self and others' hands. Cognitive, Affective, & Behavioral Neuroscience, 17(4), 826-837.

de Gelder B (2006) Towards the neurobiology of emotional body language. Nat Rev Neurosci 7:242–249.

de Gelder B (2009) Why bodies? Twelve reasons for including bodily expressions in affective neuroscience. Philos Trans R Soc Lond B Biol Sci 364:3475–3484.

Desmurget, M., Epstein, C. M., Turner, R. S., Prablanc, C., Alexander, G. E., & Grafton, S. T. (1999). Role of the posterior parietal cortex in updating reaching movements to a visual target. Nature neuroscience, 2(6), 563-567.

Devue, C., Collette, F., Balteau, E., Degueldre, C., Luxen, A., Maquet, P., & Brédart, S. (2007). Here I am: the cortical correlates of visual self-recognition. Brain research, 1143, 169-182.

Di Pellegrino, G., Fadiga, L., Fogassi, L., Gallese, V., & Rizzolatti, G. (1992). Understanding motor events: a neurophysiological study. Experimental brain research, 91(1), 176-180.

Downing, P. E., Jiang, Y., Shuman, M., & Kanwisher, N. (2001). A cortical area selective for visual processing of the human body. Science, 293(5539), 2470e2473. http://dx.doi.org/10.1126/ science.1063414.

Downing, P. E., Peelen, M. V., Wiggett, A. J., & Tew, B. D. (2006). The role of the extrastriate body area in action perception. Social Neuroscience,, 1(1), 52-62.

Downing, P. E., Chan, A. Y., Peelen, M. V., Dodds, C. M., & Kanwisher, N. (2006). Domain specificity in visual cortex. Cerebral cortex, 16(10), 1453-1461.

Ehrsson, H. H., Geyer, S., & Naito, E. (2003). Imagery of voluntary movement of fingers, toes, and tongue activates corresponding body-part-specific motor representations. Journal of neurophysiology.

Engelen, T., de Graaf, T. A., Sack, A. T., & de Gelder, B. (2015). A causal role for inferior parietal lobule in emotion body perception. cortex, 73(195), e202.

Fogassi, L., Ferrari, P. F., Gesierich, B., Rozzi, S., Chersi, F., & Rizzolatti, G. (2005). Parietal lobe: from action organization to intention understanding. Science, 308(5722), 662-667.

Friston, K. J., Buechel, C., Fink, G. R., Morris, J., Rolls, E., & Dolan, R. J. (1997). Psychophysiological and modulatory interactions in neuroimaging. Neuroimage, 6(3), 218-229.

Gallese, V., & Goldman, A. (1998). Mirror neurons and the simulation theory of mind-reading. Trends in cognitive sciences, 2(12), 493-501.

Gallese, V. (2006, October). Embodied simulation: from mirror neuron systems to interpersonal relations. In *Empathy and Fairness: Novartis Foundation Symposium 278* (pp. 3-19). Chichester, UK: John Wiley & Sons, Ltd.

Genovese, C. R., Lazar, N. A., & Nichols, T. (2002). Thresholding of statistical maps in functional neuroimaging using the false discovery rate. Neuroimage, 15(4), 870-878.

Goldenberg, G., & Spatt, J. (2009). The neural basis of tool use. *Brain*, *132*(6), 1645-1655.

Graziano, M. S., Taylor, C. S., & Moore, T. (2002). Complex movements evoked by microstimulation of precentral cortex. Neuron, 34(5), 841-851.

Graziano, M. S. (2016). Ethological action maps: a paradigm shift for the motor cortex. Trends in cognitive sciences, 20(2), 121-132.

Greve, D. N., & Fischl, B. (2009). Accurate and robust brain image alignment using boundary-based registration. Neuroimage, 48(1), 63-72.

Grèzes J, Armony JL, Rowe J, Passingham RE. Activations related to “mirror” and “canonical” neurones in the human brain: an fMRI study, Neuroimage., 2003, vol. 18 (pg. 928-937)

Haaland, K. Y., Harrington, D. L., & Knight, R. T. (2000). Neural representations of skilled movement. *Brain*, *123*(11), 2306-2313.

Haaland, K. Y. (2006). Left hemisphere dominance for movement. *The clinical neuropsychologist*, *20*(4), 609-622.

Haxby, J. V., Connolly, A. C., & Guntupalli, J. S. (2014). Decoding neural representational spaces using multivariate pattern analysis. Annual review of neuroscience, 37, 435-456.

Hodzic, A., Kaas, A., Muckli, L., Stirn, A., & Singer, W. (2009). Distinct cortical networks for the detection and identification of human body. Neuroimage, 45(4), 1264-1271.

Hohmann, T., Troje, N. F., Olmos, A., & Munzert, J. (2011). The influence of motor expertise and motor experience on action and actor recognition. Journal of Cognitive Psychology, 23(4), 403– 415.Return to ref 2011 in article

Iacoboni, M., Koski, L. M., Brass, M., Bekkering, H., Woods, R. P., Dubeau, M. C., ... & Rizzolatti, G. (2001). Reafferent copies of imitated actions in the right superior temporal cortex. Proceedings of the national academy of sciences, 98(24), 13995-13999.

Iacoboni, M., Molnar-Szakacs, I., Gallese, V., Buccino, G., Mazziotta, J. C., & Rizzolatti, G. (2005). Grasping the intentions of others with one's own mirror neuron system. PLoS biology, 3(3), e79.

Iacoboni, M. (2008). Mirroring people: The new science of how we connect with others. Farrar, Straus and Giroux.

Iacoboni, M. (2009). Imitation, empathy, and mirror neurons. Annual review of psychology, 60, 653-670.

Ionta S, Heydrich L, Lenggenhager B, Mouthon M, Fornari E, Chapuis D, Gassert R, Blanke O. Multisensory mechanisms in temporo-parietal cortex support self-location and first-person perspective. Neuron. 2011 Apr 28;70(2):363-74. doi: 10.1016/j.neuron.2011.03.009. PMID: 21521620.

Isik, L., Koldewyn, K., Beeler, D., & Kanwisher, N. (2017). Perceiving social interactions in the posterior superior temporal sulcus. *Proceedings of the National Academy of Sciences*, 114(43), E9145-E9152.

Jackson, P. L., & Decety, J. (2004). Motor cognition: A new paradigm to study self–other interactions. Current opinion in Neurobiology, 14(2), 259-263.

Jeannerod, M. Visual and action cues contribute to the self–other distinction. Nat Neurosci 7, 422– 423 (2004). https://doi.org/10.1038/nn0504-422

Jeannerod, M., & Pacherie, E. (2004). Agency, simulation and self-identification. Mind & language, 19(2), 113-146.

Jenkinson, M and Smith, S. A global optimisation method for robust affine registration of brain images. Medical Image Analysis, 5(2):143-156, 2001.

Jenkinson, M., Bannister, P., Brady, J., and Smith, S. Improved optimisation for the robust and accurate linear registration and motion correction of brain images. NeuroImage, 17(2):825-841, 2002.

Johansson, G. (1973). Visual perception of biological motion and a model for its analysis. Perception & psychophysics, 14, 201-211.

Jokisch, D., Daum, I., & Troje, N. F. (2006). Self recognition versus recognition of others by biological motion: Viewpoint-dependent effects. Perception, 35(7), 911-920.

Kadambi A, Xie Q, Lu H (2024) Individual differences and motor planning influence self-recognition of actions. PLoS ONE 19(7): e0303820. https://doi.org/10.1371/journal.pone.0303820

Kaplan, J. T., Aziz-Zadeh, L., Uddin, L. Q., & Iacoboni, M. (2008). The self across the senses: an fMRI study of self-face and self-voice recognition. *Social cognitive and affective neuroscience*, *3*(3), 218-223.

Keenan, J. P., Wheeler, M., Platek, S. M., Lardi, G., & Lassonde, M. (2003). Self-face processing in a callosotomy patient. European Journal of Neuroscience, 18(8), 2391-2395.

Keysers, C., & Gazzola, V. (2007). Integrating simulation and theory of mind: from self to social cognition. Trends in cognitive sciences, 11(5), 194-196.

Knoblich, G., & Flach, R. (2003). Action identity: Evidence from self-recognition, prediction, and coordination. Consciousness and cognition, 12(4), 620-632.

Kilner, J. M. (2011). More than one pathway to action understanding. Trends in cognitive sciences, 15(8), 352-357.

Kilteni K, Ehrsson HH (2024). Dynamic changes in somatosensory and cerebellar activity mediate temporal recalibration of self-touch. Commun Biol. 2024 May 3;7(1):522. doi: 10.1038/s42003-024-06188-4.

Kilteni K, Engeler P, Boberg I, Maurex L, Ehrsson HH (2021). No evidence for somatosensory attenuation during action observation of self-touch. Eur J Neurosci. 2021 Oct;54(7):6422-6444. doi: 10.1111/ejn.15436.

Kilteni K, Andersson BJ, Houborg C, Ehrsson HH (2018). Motor imagery involves predicting the sensory consequences of the imagined movement. Nat Commun. 2018 Apr 24;9(1):1617. doi: 10.1038/s41467-018-03989-0. PMID: 29691389; PMCID: PMC5915435.

Kirsch, L. P., & Cross, E. S. (2015). Additive routes to action learning: layering experience shapes engagement of the action observation network. Cerebral Cortex, 25(12), 4799-4811.

Koski, L., Iacoboni, M., Dubeau, M. C., Woods, R. P., & Mazziotta, J. C. (2003). Modulation of cortical activity during different imitative behaviors. Journal of neurophysiology.

Krachun, C., Lurz, R., Mahovetz, L. M., & Hopkins, W. D. (2019). Mirror self-recognition and its relationship to social cognition in chimpanzees. Animal Cognition, 22, 1171-1183.

Kriegeskorte, N., Mur, M., & Bandettini, P. A. (2008). Representational similarity analysis connecting the branches of systems neuroscience. Frontiers in systems neuroscience, 2, 4.

Lamm, C., Fischer, M. H., & Decety, J. (2007). Predicting the actions of others taps into one's own somatosensory representations—a functional MRI study. Neuropsychologia, 45(11), 2480-2491.

Leung, H. C., & Cai, W. (2007). Common and differential ventrolateral prefrontal activity during inhibition of hand and eye movements. Journal of Neuroscience, 27(37), 9893-9900.

Leshinskaya, A., & Caramazza, A. (2014). Nonmotor aspects of action concepts. Journal of Cognitive Neuroscience, 26(12), 2863-2879.

Liakakis, G., Nickel, J., & Seitz, R. (2011). Diversity of the inferior frontal gyrus—a meta-analysis of neuroimaging studies. Behavioural brain research, 225(1), 341-347.

Lieberman, M. D., Straccia, M. A., Meyer, M. L., Du, M., & Tan, K. M. (2019). Social, self,(situational), and affective processes in medial prefrontal cortex (MPFC): Causal, multivariate, and reverse inference evidence. Neuroscience & Biobehavioral Reviews, 99, 311328.

Limanowski, J., & Blankenburg, F. (2016). Integration of visual and proprioceptive limb position information in human posterior parietal, premotor, and extrastriate cortex. Journal of Neuroscience, 36(9), 2582-2589.

Lingnau, A., & Downing, P. E. (2015). The lateral occipitotemporal cortex in action. Trends in cognitive sciences, 19(5), 268-277.

Lombardo, M. V., Chakrabarti, B., Bullmore, E. T., Wheelwright, S. J., Sadek, S. A., Suckling, J., ... & Baron-Cohen, S. (2010). Shared neural circuits for mentalizing about the self and others. Journal of cognitive neuroscience, 22(7), 1623-1635.

Loula, F., Prasad, S., Harber, K., & Shiffrar, M. (2005). Recognizing people from their movement. Journal of Experimental Psychology: Human Perception and Performance, 31(1), 210.

Macaluso, E., & Driver, J. (2005). Multisensory spatial interactions: a window onto functional integration in the human brain. *Trends in Neurosciences, 28*(5), 264-271.

Macuga, K. L., & Frey, S. H. (2011). Selective responses in right inferior frontal and supramarginal gyri differentiate between observed movements of oneself vs. another. Neuropsychologia, 49(5), 1202-1207.

McLaren, D. G., Ries, M. L., Xu, G., & Johnson, S. C. (2012). A generalized form of contextdependent psychophysiological interactions (gPPI): a comparison to standard approaches. Neuroimage, 61(4), 1277-1286.

Molnar-Szakacs, I., & Uddin, L. Q. (2013). Self-processing and the default mode network: interactions with the mirror neuron system. Frontiers in human neuroscience, 7, 571.

Morin, A., & Michaud, J. (2007). Self-awareness and the left inferior frontal gyrus: inner speech use during self-related processing. Brain research bulletin, 74(6), 387-396.

Morita, T., Tanabe, H. C., Sasaki, A. T., Shimada, K., Kakigi, R., & Sadato, N. (2014). The anterior insular and anterior cingulate cortices in emotional processing for self-face recognition. Social cognitive and affective neuroscience, 9(5), 570-579.

Muir, R. B., & Lemon, R. N. (1983). Corticospinal neurons with a special role in precision grip. Brain research, 261(2), 312-316.

Mukamel, R., Ekstrom, A. D., Kaplan, J., Iacoboni, M., & Fried, I. (2010). Single-neuron responses in humans during execution and observation of actions. Current biology, 20(8), 750756.

Mumford, J., Turner, B., Ashby, G., & Poldrack, R. (2012). Deconvolving BOLD activation in event-related designs for multivoxel pattern classification analyses. Neuroimage, 59(3), 2636–2643. doi: 10.1016/j.neuroimage.2011.08.076

Nichols, T., Brett, M., Andersson, J., Wager, T., & Poline, J. B. (2005). Valid conjunction inference with the minimum statistic. Neuroimage, 25(3), 653-660.

Oosterhof, N. N., Connolly, A. C., & Haxby, J. V. (2016). CoSMoMVPA: multi-modal multivariate pattern analysis of neuroimaging data in Matlab/GNU Octave. Frontiers in neuroinformatics, 10, 27.

Orgs G, Dovern A, Hagura N, Haggard P, Fink GR, Weiss PH (2016) Constructing visual perception of body movement with the motor cortex. Cereb Cortex 26:440–449

Peelen, M. V., & Downing, P. E. (2005). Selectivity for the human body in the fusiform gyrus. Journal of neurophysiology, 93(1), 603-608.

Pereira, F., & Botvinick, M. (2011). Information mapping with pattern classifiers: a comparative study. Neuroimage, 56(2), 476-496.

Pfurtscheller, G., & Neuper, C. (1997). Motor imagery activates primary sensorimotor area in humans. Neuroscience letters, 239(2-3), 65-68.

Pilgramm, S., de Haas, B., Helm, F., Zentgraf, K., Stark, R., Munzert, J., & Krüger, B. (2016). Motor imagery of hand actions: Decoding the content of motor imagery from brain activity in frontal and parietal motor areas. Human brain mapping, 37(1), 81-93.

Platek, S. M., Wathne, K., Tierney, N. G., & Thomson, J. W. (2008). Neural correlates of self-face recognition: an effect-location meta-analysis. Brain research, 1232, 173-184.

Platek, S. M., Loughead, J. W., Gur, R. C., Busch, S., Ruparel, K., Phend, N., ... & Langleben, D. D. (2006). Neural substrates for functionally discriminating self-face from personally familiar faces. Human brain mapping, 27(2), 91-98.

Porro, C. A., Cettolo, V., Francescato, M. P., & Baraldi, P. (2000). Ipsilateral involvement of primary motor cortex during motor imagery. European Journal of Neuroscience, 12(8), 3059-3063.

Price, C. J., & Friston, K. J. (1997). Cognitive conjunction: a new approach to brain activation experiments. Neuroimage, 5(4), 261-270.

Qin, P., & Northoff, G. (2011). How is our self related to midline regions and the default-mode network?. Neuroimage, 57(3), 1221-1233.

Qin, P., Wang, M., & Northoff, G. (2020). Linking bodily, environmental and mental states in the self—A three-level model based on a meta-analysis. Neuroscience & biobehavioral reviews, 115, 77-95.

Raine, A. (1991). The spq: A scale for the assessment of schizotypal personality based on DSMIII-r criteria. *Schizophrenia Bulletin*. https://doi.org/10.1093/schbul/17.4.555

Roberts, R., Callow, N., Hardy, L., Markland, D., & Bringer, J. (2008). Movement imagery ability: development and assessment of a revised version of the vividness of movement imagery questionnaire. Journal of Sport and Exercise Psychology, 30(2), 200-221.

Rissman, J., Gazzaley, A., & D'Esposito, M. (2004). Measuring functional connectivity during distinct stages of a cognitive task. Neuroimage, 23(2), 752-763.

Rizzolatti, G., & Craighero, L. (2004). The mirror-neuron system. Annu. Rev. Neurosci., 27, 169192.

Rizzolatti, G., Fadiga, L., Gallese, V., & Fogassi, L. (1996). Premotor cortex and the recognition of motor actions. Cognitive brain research, 3(2), 131-141.

Rizzolatti, G., Cattaneo, L., Fabbri-Destro, M., & Rozzi, S. (2014). Cortical mechanisms underlying the organization of goal-directed actions and mirror neuron-based action understanding. Physiological reviews, 94(2), 655-706.

Roberts, R., Callow, N., Hardy, L., Markland, D., & Bringer, J. (2008). Movement imagery ability: Development and assessment of a revised version of the vividness of movement imagery questionnaire. *Journal of Sport and Exercise Psychology*. https://doi.org/10.1123/jsep.30.2.200

Sasaki, A. T., Okamoto, Y., Kochiyama, T., Kitada, R., & Sadato, N. (2018). Distinct sensitivities of the lateral prefrontal cortex and extrastriate body area to contingency between executed and observed actions. Cortex, 108, 234–251.

Saygin, A. P., & Dick, F. (2014). The emergence of mirror-like response properties from domaingeneral principles in vision and audition. Behavioral and brain sciences, 37(2), 219.

Schmidt, Richard A. "A schema theory of discrete motor skill learning." Psychological review 82.4 (1975): 225.

Seeley, W. W., Menon, V., Schatzberg, A. F., Keller, J., Glover, G. H., Kenna, H., ... & Greicius, M. D. (2007). Dissociable intrinsic connectivity networks for salience processing and executive control. Journal of Neuroscience, 27(9), 2349-2356.

Smith, S. M., & Nichols, T. E. (2009). Threshold-free cluster enhancement: addressing problem of smoothing, threshold dependence and localisation in cluster inference. Neuroimage, 44(1), 8398.

Soch, J., Deserno, L., Assmann, A., Barman, A., Walter, H., Richardson-Klavehn, A., & Schott, B. H. (2017). Inhibition of information flow to the default mode network during self-reference versus reference to others. Cerebral Cortex, 27(8), 3930-3942.

Sokolov AA, Zeidman P, Erb M, Ryvlin P, Friston KJ, Pavlova, MA. 2018. Structural and effective brain connectivity underlying biological motion detection. Proc Natl Acad Sci U S A. 115:E12034–E12042.

Sperry, R. W., Zaidel, E., & Zaidel, D. (1979). Self recognition and social awareness in the deconnected minor hemisphere. *Neuropsychologia*, *17*(2), 153-166.

Sperduti, M, P. Delaveau, P. Fossati, J. Nadel (2011) Different brain structures related to self- and external-agency attribution: A brief review and meta-analysis. Brain Structure and Function, 216 (2011), pp. 151-157

Stetson, C., Cui, X., Montague, P. R. & Eagleman, D. M. Motor-sensory recalibration leads to an illusory reversal of action and sensation. Neuron 51, 651-659 (2006)

Sugiura, M., Kawashima, R., Nakamura, K., Okada, K., Kato, T., Nakamura, A., ... & Fukuda, H. (2000). Passive and active recognition of one's own face. *Neuroimage*, 11(1), 36-48.

Sugiura, M., Watanabe, J., Maeda, Y., Matsue, Y., Fukuda, H., & Kawashima, R. (2005). Cortical mechanisms of visual self-recognition. Neuroimage, 24(1), 143-149.

Sugiura, M., Sassa, Y., Jeong, H., Miura, N., Akitsuki, Y., Horie, K., ... & Kawashima, R. (2006). Multiple brain networks for visual self-recognition with different sensitivity for motion and body part. *Neuroimage*, 32(4), 1905-1917.

Sui, J., & Gu, X. (2017). Self as object: Emerging trends in self research. Trends in neurosciences, 40(11), 643-653.

Tacikowski P, Berger CC, Ehrsson HH. Dissociating the Neural Basis of Conceptual Self-Awareness from Perceptual Awareness and Unaware Self-Processing. Cereb Cortex. 2017 Jul 1;27(7):3768-3781. doi: 10.1093/cercor/bhx004.

Tholen, M. G., Schurz, M., & Perner, J. (2019). The role of the IPL in person identification. Neuropsychologia, 129, 164-170.

Turk DJ, Heatherton TF, Kelley WM, Funnell MG, Gazzaniga MS, Macrae CN (2002) Mike or me? Self-recognition in a split brain patient. Nat Neurosci 5:841–842

Turk, D. J., Heatherton, T. F., Macrae, C. N., Kelley, W. M., & Gazzaniga, M. S. (2003). Out of contact, out of mind: the distributed nature of the self. Annals of the New York Academy of Sciences, 1001(1), 65-78.

Uddin, L. Q. (2016). Salience network of the human brain. Academic press.

Uddin, L. Q., Kaplan, J. T., Molnar-Szakacs, I., Zaidel, E., & Iacoboni, M. (2005). Self-face recognition activates a frontoparietal “mirror” network in the right hemisphere: an event-related fMRI study. *Neuroimage*, *25*(3), 926-935.

Uddin, L. Q., Rayman, J., & Zaidel, E. (2005). Split-brain reveals separate but equal selfrecognition in the two cerebral hemispheres. *Consciousness and cognition*, *14*(3), 633-640.

Uddin, L. Q., Iacoboni, M., Lange, C., & Keenan, J. P. (2007). The self and social cognition: the role of cortical midline structures and mirror neurons. *Trends in cognitive sciences*, *11*(4), 153157.

Uhlmann, L., Pazen, M., van Kemenade, B. M., Steinsträter, O., Harris, L. R., Kircher, T., & Straube, B. (2020). Seeing your own or someone else's hand moving in accordance with your action: The neural interaction of agency and hand identity. Human brain mapping, 41(9), 24742489.

Ürgen, B. A., Pehlivan, S., & Saygin, A. P. (2019). Distinct representations in occipito-temporal, parietal, and premotor cortex during action perception revealed by fMRI and computational modeling. Neuropsychologia, 127, 35-47.

Urgesi, C., Candidi, M., Ionta, S., & Aglioti, S. M. (2007). Representation of body identity and body actions in extrastriate body area and ventral premotor cortex. *Nature neuroscience*, *10*(1), 30-31.

van Boxtel, J. J., & Lu, H. (2013). A biological motion toolbox for reading, displaying, and manipulating motion capture data in research settings. Journal of vision, 13(12), 7-7.

Van Den Bos, E., and Jeannerod, M. (2002). Sense of body and sense of action both contribute to self-recognition. *Cognition* 85, 177–187. doi: 10.1016/S0010-0277(02)00100-2

van Kemenade, B. M., Arikan, B. E., Kircher, T., & Straube, B. (2017). The angular gyrus is a supramodal comparator area in action–outcome monitoring. Brain Structure and Function, 222(8), 3691-3703.

Van Kemenade, B. M., Arikan, E. A., Podranski, K., Steinsträter, O., Kircher, T., & Straube, B. (2019). Distinct roles for the cerebellum, angular gyrus and middle temporal gyrus in actionfeedback monitoring. Cerebral Cortex, 29, 1520–1531. https://doi.org/10.1093/cercor/bhy048

van Veluw, S. J., & Chance, S. A. (2014). Differentiating between self and others: an ALE metaanalysis of fMRI studies of self-recognition and theory of mind. *Brain imaging and behavior*, *8*(1), 24-38.

Vocks, S., Busch, M., Grönemeyer, D., Schulte, D., Herpertz, S., & Suchan, B. (2010). Differential neuronal responses to the self and others in the extrastriate body area and the fusiform body area. Cognitive, Affective, & Behavioral Neuroscience, 10(3), 422-429.

Weiner, K. S., & Grill-Spector, K. (2011). Not one extrastriate body area: using anatomical landmarks, hMT+, and visual field maps to parcellate limb-selective activations in human lateral occipitotemporal cortex. Neuroimage, 56(4), 2183-2199.

Winkler, A. M., Ridgway, G. R., Webster, M. A., Smith, S. M., & Nichols, T. E. (2014). Permutation inference for the general linear model. *Neuroimage*, *92*, 381-397.

Worsley, K. J. (2001). Statistical analysis of activation images. Functional MRI: An introduction to methods, 14(1), 251-70.

Woźniak, M., Schmidt, T. T., Wu, Y. H., Blankenburg, F., & Hohwy, J. (2022). Differences in working memory coding of biological motion attributed to oneself and others. *Human Brain Mapping.*

Wurm, M. F., & Caramazza, A. (2021). Two 'what'pathways for action and object recognition. *Trends in cognitive sciences*.

Wurm, M. F., & Lingnau, A. (2015). Decoding Actions at Different Levels of Abstraction. *Journal of Neuroscience,* 35(20), 7727–7735. https://doi.org/10.1523/JNEUROSCI.0188-15.2015

Wurm, M. F., Caramazza, A., & Lingnau, A. (2017). Action categories in lateral occipitotemporal cortex are organized along sociality and transitivity. *Journal of Neuroscience*, 37(3), 562-575.

Yeshurun, Y., Nguyen, M., & Hasson, U. (2021). The default mode network: where the idiosyncratic self meets the shared social world. *Nature reviews neuroscience*, 22(3), 181-192.

Yovel, G., & O'Toole, A. J. (2016). Recognizing people in motion. *Trends in cognitive sciences*, 20(5), 383-395.

Figure captions

Fig 1. **Trial structure including timing.** Participants centrally attended to a white fixation cross until the action (self/friend/other) appeared for 5 s. On a subsequent screen, participants were then provided 2 s to make their identity judgment, followed by the variable ITI (mean-centered at 5 s). The response order of self, friend, other was counterbalanced in order to reduce any impact of motor order.

Fig 2. *Left Panel:* Representational (dis)similarity matrices (RDMs) used for each representational dissimilarity analysis averaged across participants. RDMs reflect the Euclidean distance between identity and action categories for speed, movement distinctiveness and body structure. For motor familiarity, identity was based on the degree of motor dissimilarity to oneself (self-generated actions, i.e., verbal instruction: zero dissimilarity; self-imitated actions, i.e., visual instruction: small dissimilarity, 0.3; friend actions: medium dissimilarity, 0.6; strangers: most dissimilarity, 1). Brighter colors for all RDMs indicate more dissimilarity. *Top Right Panel:* Upper triangular pairwise dissimilarity (1 – spearman's rho) between each of the group-level RDMs. Brighter colors indicate more dissimilarity. *Bottom Right Panel:* DTW figure showing movement trajectory of one joint from one actor's action time series (shown as red dots indicating locations) with lines measuring similarity to the corresponding joint in another actor's time series (shown as green dots) to find the optimal decrease in dissimilarity over time.

Fig 3. **Behavioral results of identity recognition accuracy.** *Top:* Self-recognition performance for different actions color coded by action type (verbal instruction: gray; visual instruction: blue). Light gray fill indicates bar plots for verbal instruction. Light blue fill indicates bar plot for visual instruction. Inference bands denote 95% Bayesian highest density interval with 1000 iterations. Horizontal blue line indicates chance-level recognition accuracy (.33). *Bottom left panel*: depicts confusion matrix for each identity. No significant misattributions were found for the self relative to other identities, though friend and stranger were more confused relative to the self (~55% increase in misattributions for friend and strangers). *Bottom right panel*: average recognition accuracy for each identity. All identities were recognized significantly above chance. Self actions were recognized significantly better than friend actions. Light gray fill indicates bar plots. Inference bands denote 95% Bayesian highest density interval with 1000 iterations. Horizontal blue line indicates chance-level recognition accuracy (.33). * $p < .05$, ** $p < .01$, *** $p < .001$.

Fig 4. Group-level activity obtained using FSL's non-parametric permutation approach (*randomise*) with TFCE, $p < .05$. *From Left to Right:* Self v baseline; friend v baseline; and stranger v baseline.

$^{+}$ Large cluster sizes were obtained with TFCE due to the optimal cluster-defining threshold; hence cluster peaks are reported with visual interpolation using manual thresholding with a sliding scale. *Abbreviations*: Inferior Frontal Cortex (IFC); Superior Temporal Sulcus (STS); Lateral Occipital Cortex (LOC); Supplementary Motor Area (SMA); Supramarginal Gyrus (SMG); Angular Gyrus (Ang).

Fig 5. Univariate group-level activity for *self > stranger* (left) and *self > friend* (right) using the FSL *randomise* permutation approach, cluster corrected with TFCE ($p < .05$). Violin plot shows mean parameter estimates (PE) for the left posterior supramarginal gyrus (SMG) for all identities. The left SMG significantly discriminated contrasts of PE for both self vs stranger ($p = .001$) and self vs friend ($p = .005$), but not friend vs stranger ($p = .821$). Extended Data Figures 5-1 and 5-3 report the activity maps and peak clusters for both TFCE contrasts, as well as RFT cluster-corrected results (Figures 5-2 and 5-5).

Fig 6. Task-modulated functional connectivity of left and right IPL. Left IPL (top panel) seed showed increased connectivity with bilateral occipito-temporal regions, bilateral superior and inferior parietal areas, and bilateral inferior frontal cortex during *self* > *stranger.* For *self* > *friend*, functional connectivity analysis revealed greater connectivity with the bilateral inferior frontal cortices and occipito-temporal regions. Task-modulated functional connectivity of the right IPL (bottom panel) showed a similar activity pattern to the left: strengthened fronto-parietal and parieto-occipital connectivity for both contrasts. All activity cluster corrected at $Z > 2.3$, $p < .01$. Abbreviations: IPL (Inferior Parietal Lobule), IPS (Intraparietal Sulcus), IFC (Inferior Frontal Cortex), OT (Occipito-Temporal Regions), EBA (Extrastriate Body Area), STS (Superior Temporal Sulcus).

Fig 7. Multiple regression searchlight RDA results for motor familiarity. This figure depicts the z-transformed activity map for significant correlations between the motor familiarity RDM and the neural RDM based on activity patterns for actions (self encoded as least dissimilar, with action separation to account for motor familiarity between action types; friend as medium dissimilarity, stranger as most), after accounting for speed and movement distinctiveness (DTW). Activation map reflects brain activity after 10000 non-parametric Monte Carlo simulations, using TFCE and p < 0.01. *Regions:* bilateral somato-motor cortex: primary motor cortex, primary somatosensory cortex, superior parietal lobule; frontoparietal cortex: inferior parietal lobule, inferior frontal cortex, medial prefrontal cortex; occipito-temporal cortex: inferior temporal cortex, superior temporal sulcus and gyrus. All activity patterns are reported in Extended Data Table 7-1.

Fig 8. Multiple regression searchlight RDA results for each identity (self, friend, stranger). Activation maps reflect TFCE-corrected brain activity after 10000 non-parametric Monte Carlo simulations, $p < 0.01$ for self and friend; $p < .05$ for stranger. Dissimilarity matrices reflect dissimilarity based on identity across all actions. *Regions:* Frontoparietal: Inferior Parietal lobule; Superior Frontal Gyrus, lateral and medial prefrontal cortices. Somatomotor: Primary Motor Cortex (M1), Primary Somatosensory Cortex (S1). Occipito-Temporal: Superior Temporal Sulcus, Middle Temporal Gyrus, Extrastriate Body Area. Activity patterns are reported in Extended Data Tables 8-1, 8-2, 8-3, 8-4 and Figure 8-1.

Fig 9. Multiple regression searchlight RDA results for self identity, regressing out motor responses. Activation maps reflect TFCE-corrected brain activity after 10000 non-parametric Monte Carlo simulations, $p < 0.01$ for self. Dissimilarity matrix reflects dissimilarity based on self-identity across all actions. *Regions:* Frontoparietal: Inferior Parietal lobule; Superior Frontal Gyrus, lateral and medial prefrontal cortices. Somatomotor: Primary Motor Cortex (M1), Primary Somatosensory Cortex (S1). Occipito-Temporal: Superior Temporal Sulcus, Middle Temporal Gyrus, Extrastriate Body Area. Activity patterns are reported in Extended Data Table 9-1.

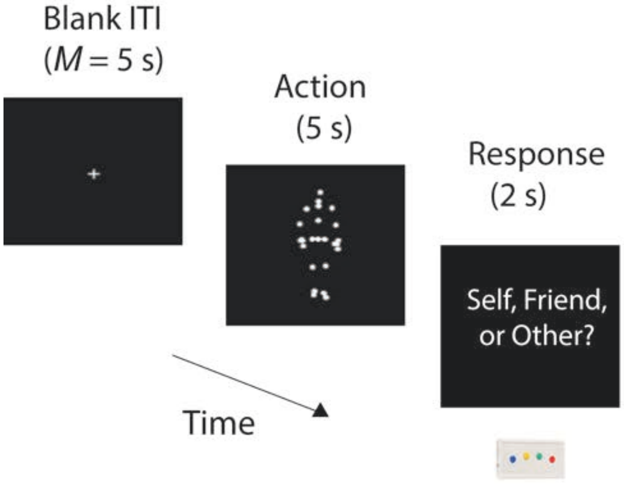

Action Types

Verbal Instruction (6): Stretch, Guitar, Hurry Up, Get Attention, Wash Windows

Visual Instruction (6): Jumping Jacks, Direct Traffic, Laughing, Basketball, Chopping, Digging

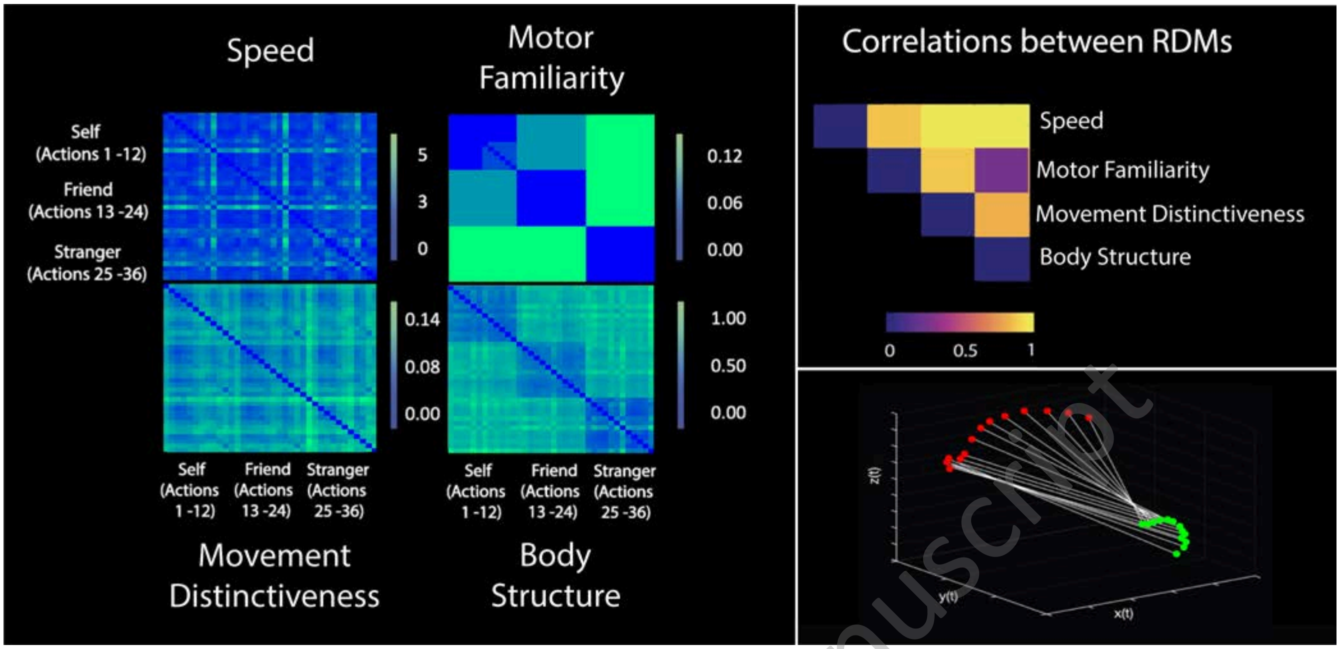
Speed
Motor Familiarity
Self (Actions 1 -12)
Friend (Actions 13 -24)
Stranger (Actions 25 -36)
5
3
0
0.12
0.06
0.00
0.14
0.08
0.00
1.00
0.50
0.00
Self (Actions 1 -12)
Friend (Actions 13 -24)
Stranger (Actions 25 -36)
Self (Actions 1 -12)
Friend (Actions 13 -24)
Stranger (Actions 25 -36)
Movement Distinctiveness
Body Structure
Correlations between RDMs
Speed
Motor Familiarity
Movement Distinctiveness
Body Structure
0
0.5
1
z(t)
y(t)
x(t)

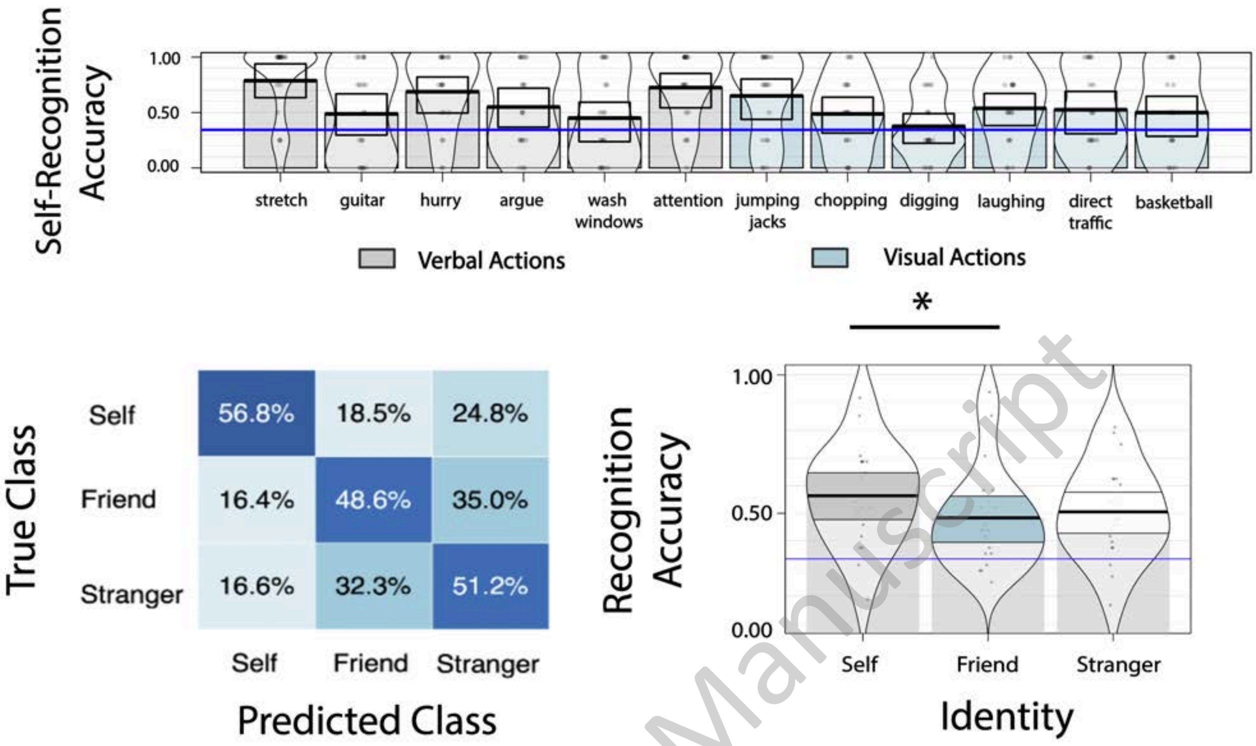
Self-Recognition Accuracy
1.00
0.50
0.00
stretch
guitar
hurry
argue
wash windows
attention
jumping jacks
chopping
digging
laughing
direct traffic
basketball
Verbal Actions
Visual Actions
True Class
Self
Friend
Stranger
56.8%
18.5%
24.8%
16.4%
48.6%
35.0%
16.6%
32.3%
51.2%
Self
Friend
Stranger
Predicted Class
*
Recognition Accuracy
1.00
0.50
0.00
Self
Friend
Stranger
Identity

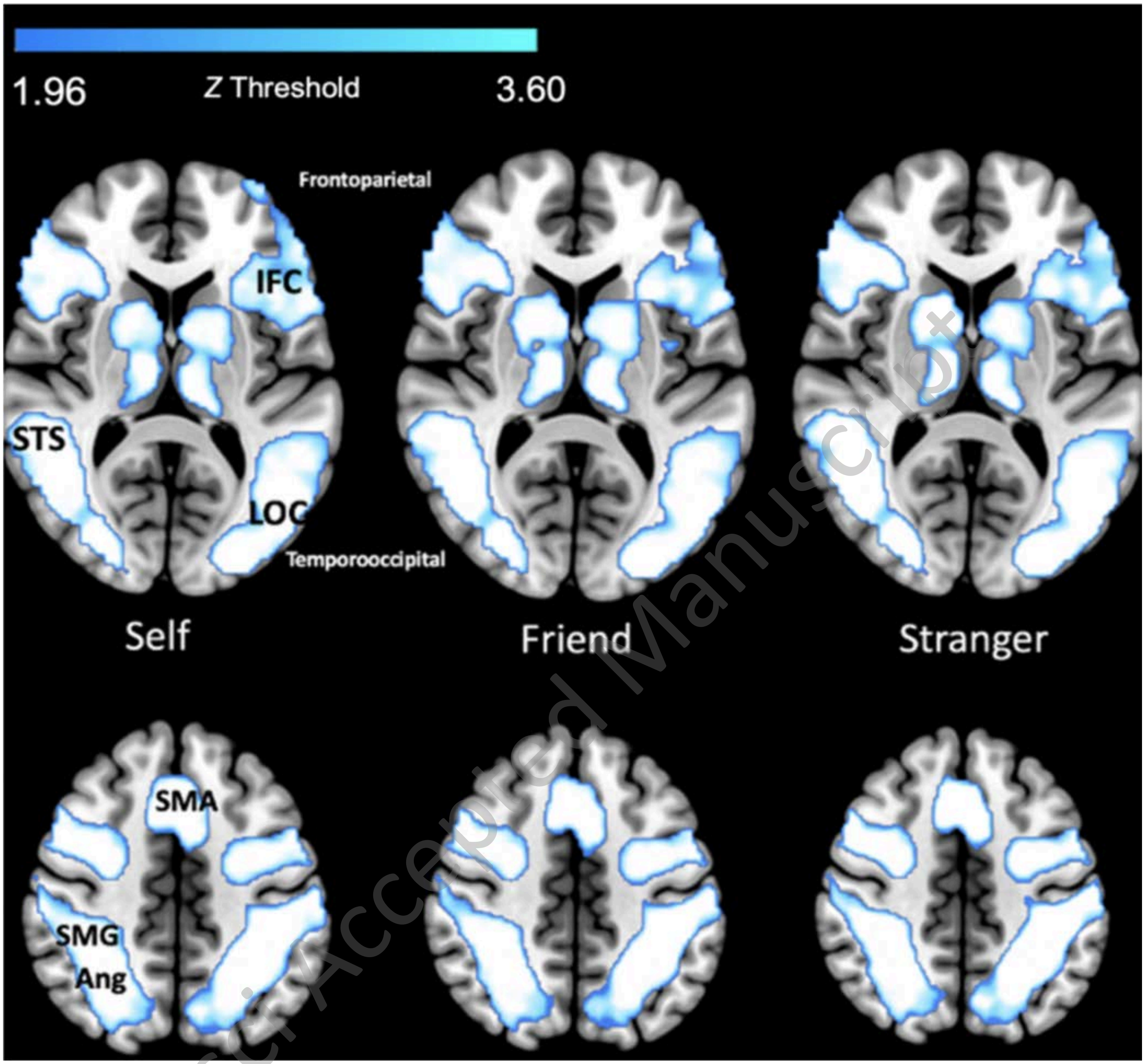
1.96
Z Threshold
3.60
Frontoparietal
IFC
STS
LOC
Temporooccipital
Self
Friend
Stranger
SMA
SMG
Ang

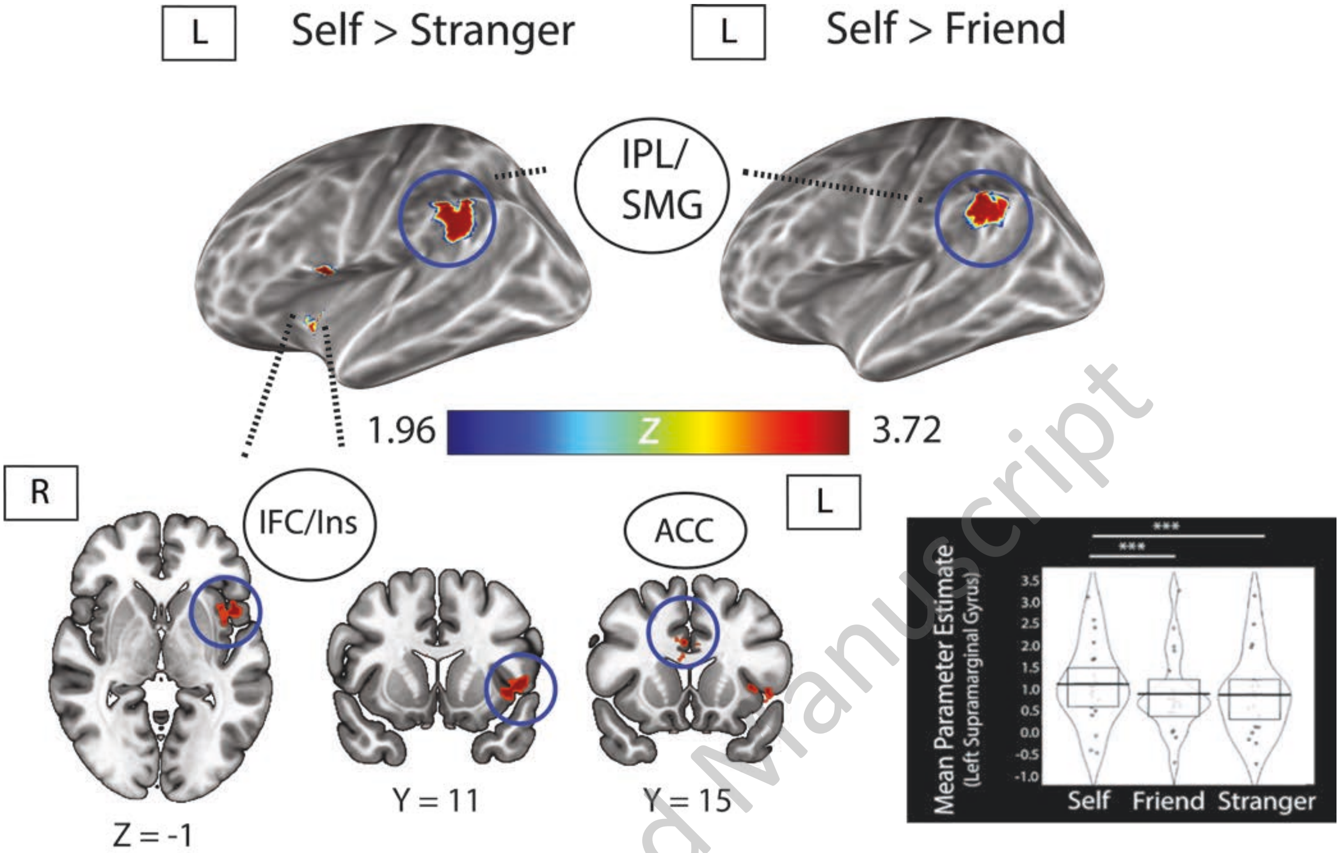
L
Self > Stranger
L
Self > Friend
IPL/
SMG
1.96
Z
3.72
R
IFC/Ins
ACC
L
Z = -1
Y = 11
Y = 15
***
***
Mean Parameter Estimate
(Left Supramarginal Gyrus)
3.5
3.0
2.5
2.0
1.5
1.0
0.5
0.0
-0.5
-1.0
Self
Friend
Stranger

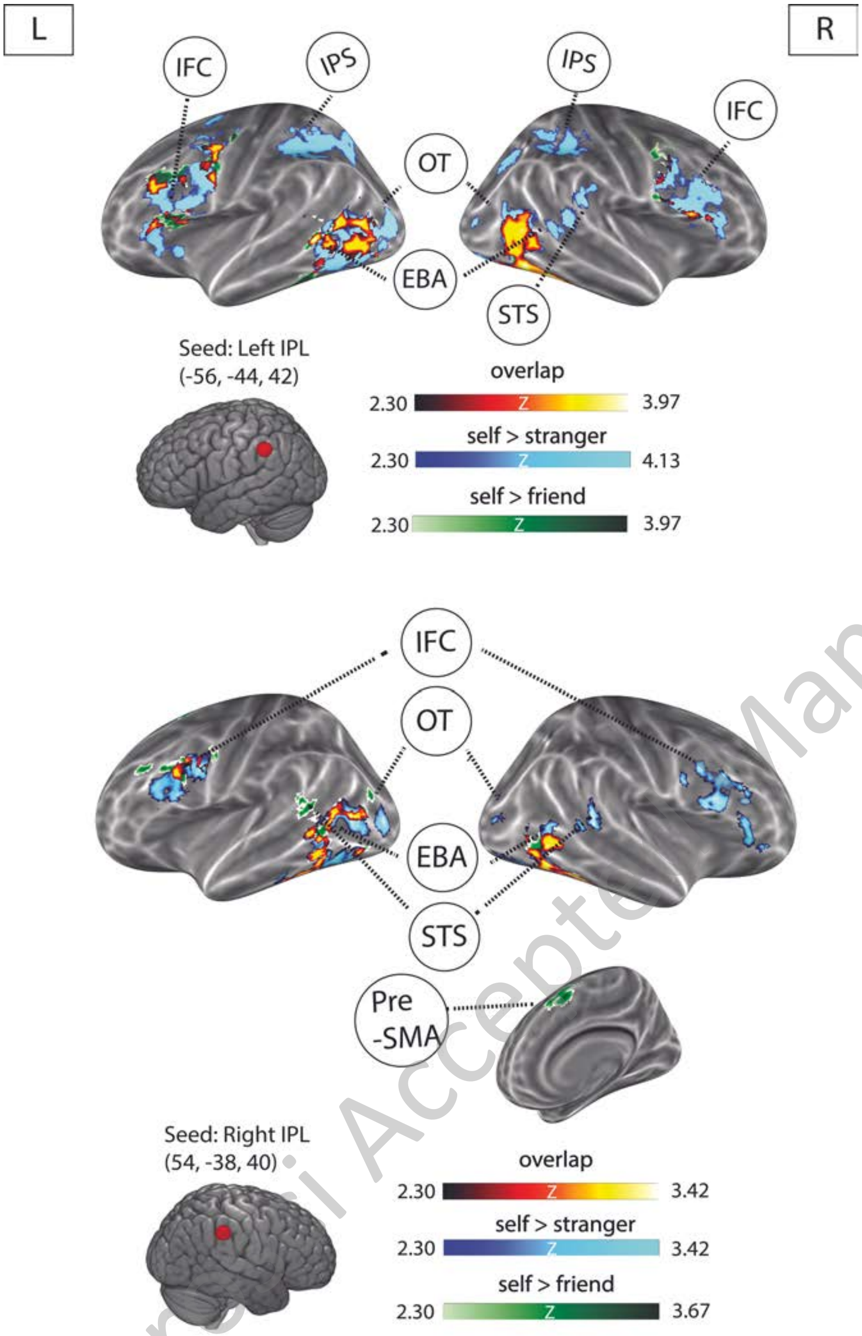
L
R
IFC
IPS
IPS
IFC
OT
EBA
STS
Seed: Left IPL
(-56, -44, 42)
overlap
2.30
Z
3.97
self > stranger
2.30
Z
4.13
self > friend
2.30
Z
3.97
IFC
OT
EBA
STS
Pre
-SMA
Seed: Right IPL
(54, -38, 40)
overlap
2.30
Z
3.42
self > stranger
2.30
Z
3.42
self > friend
2.30
Z
3.67

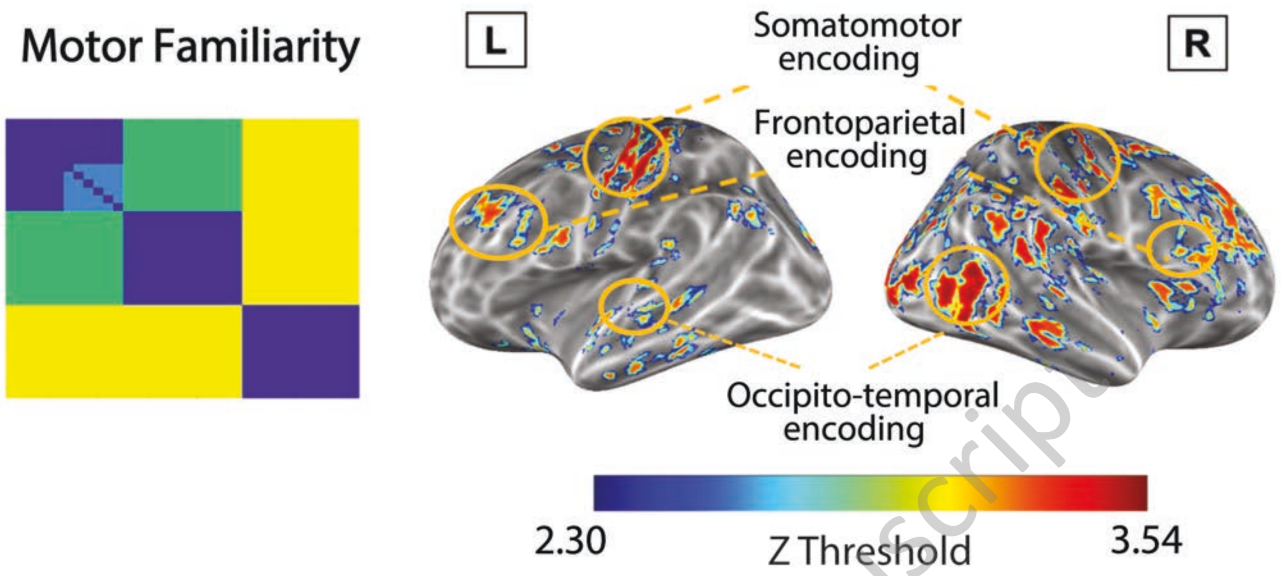
Motor Familiarity
L
R
Somatomotor encoding
Frontoparietal encoding
Occipito-temporal encoding
2.30
Z Threshold
3.54

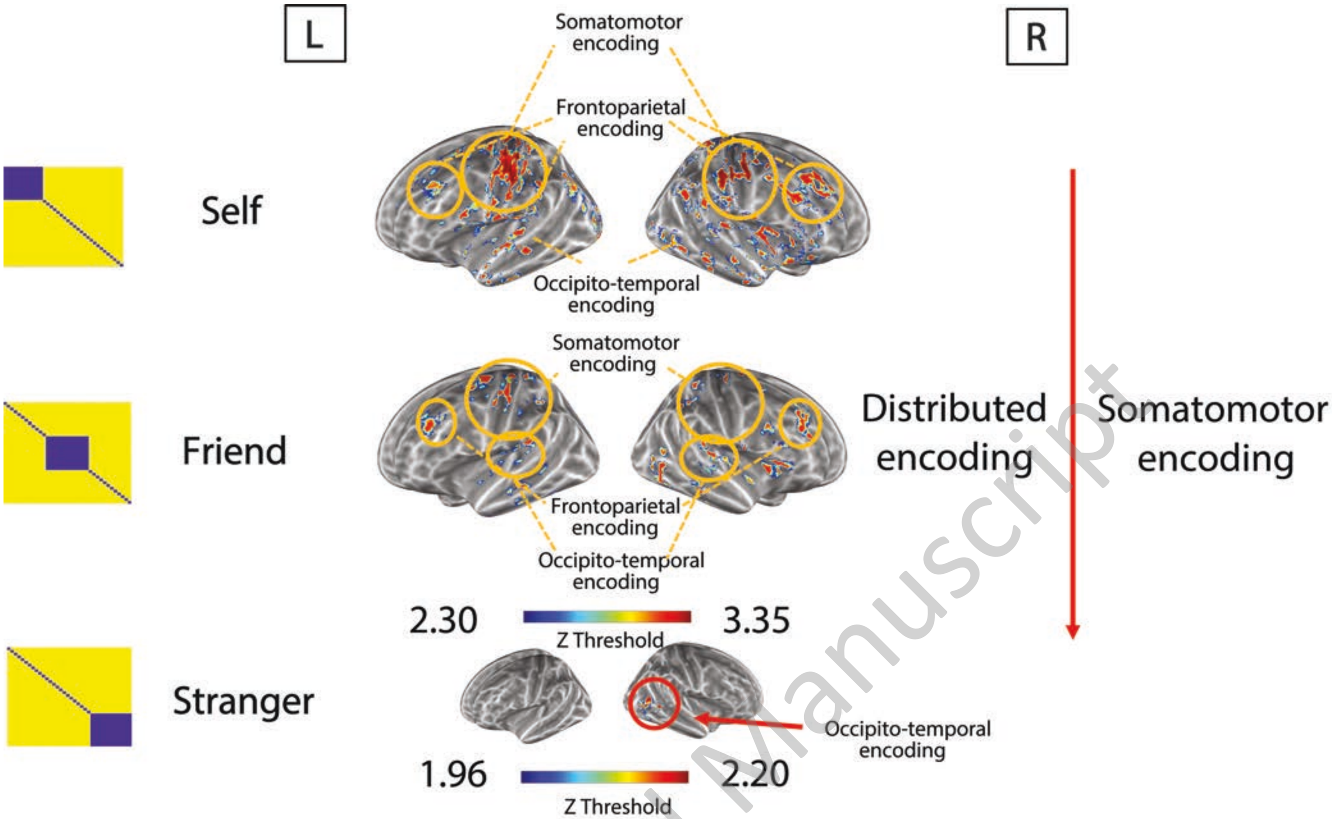
L
R
Somatomotor encoding
Frontoparietal encoding
Self
Occipito-temporal encoding
Somatomotor encoding
Friend
Distributed encoding
Somatomotor encoding
Frontoparietal encoding
Occipito-temporal encoding
2.30
3.35
Z Threshold
Stranger
Occipito-temporal encoding
1.96
2.20
Z Threshold

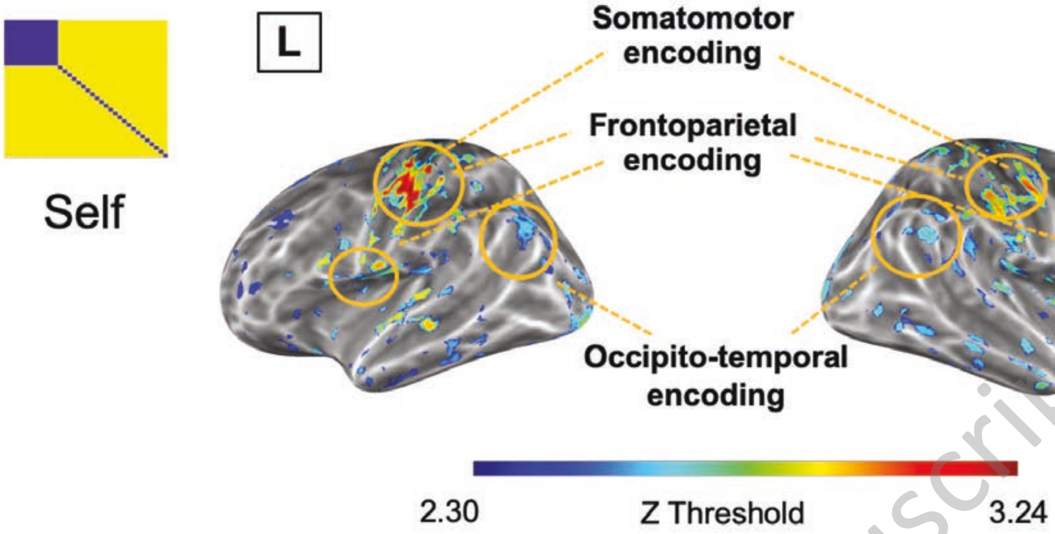
Self
L
R
Somatomotor encoding
Frontoparietal encoding
Occipito-temporal encoding
2.30
Z Threshold
3.24